Diogo Filipe Cabrita Prata
Licenciatura em Genética e Biotecnologia

Regeneration Studies in the African Spiny Mouse

Dissertação para obtenção do Grau de Mestre em
Genética Molecular e Biomedicina

Orientador: Gustavo Tiscórnia, Professor Auxiliar, Departamento de Ciencias Biomédicas e Medicina, Center for Biomedical Research, University of Algarve

FACULDADE DE CIÊNCIAS E TECNOLOGIA
UNIVERSIDADE NOVA DE LISBOA

Outubro, 2017

Statement of Authorship

The experimental work presented in this thesis have been performed by the defendant of the Master's Thesis. All work was conducted in the University of Algarve, within the research group of Molecular and Regenerative Medicine Laboratory.

Acknowledgments

I must first express my gratitude to Dr. Gustavo Tiscornia, who accepted me into his research group and helped me to better understand what a scientific career truly entails, all the sacrifices and to savor the good aspects of science, although few and brief.

I am thankful to the Coordinator of the Master in Molecular Genetics and Biomedicine, Professora Paula Gonçalves, for her guidance and patience.

Special thanks to Dr. Ashley Seifert and his colleague Dr. Thomas Gawriluk for his help and materials provided.

I am very grateful to my mentor and close friend Dino Matias, for not only steering me in the right way, but for also being a great contribution in turning dull moments into risible ones.

To the colleagues and friends that I've made during my stay in Gambelas, Gil Carraco, Ignasi Casanellas, Daniel Oliveira, Susana Machado, Gonçalo Pinheiro, Om Rathore, Adélia Ova, Marta Vitorino, Pedro Almeida, Neuton Gorjão, Daniela Baltazar, Om Rathore and Adélia Ova, my sincerest apologies for addressing as a group, I am very thankful to each one of you for the advice and the good times spent together, they made the hardest times more bearable and the good times more enjoyable.

Last, but never least, I am thankful to my mother, sister and nephews, who have supported and helped me throughout my academic progression, and always believed I could make it through the hardships. And also to my closest friend Tom Miron, every man should be so fortunate to have such a good friend to pick you up when things don't work.

Abstract

Across the Metazoa, organisms vary in terms of how they respond to injury. The two basic responses are regeneration or fibrotic scarring. While some groups such as axolotls, amphibians and fish show high regenerative capacity, mammals tend to heal wounds by fibrotic scarring. The African Spiny Mouse (*Acomys*) has been reported to have the capacity of closing 4-mm full thickness wounds in the ear pinna with full regeneration of the original tissue architecture, including dermis, epidermis, cartilage and hair follicles. In contrast, *Mus musculus* heals the border wounds by fibrotic scarring. Therefore, *Acomys* and *Mus* constitute a powerful comparative framework for the study of mammalian regeneration.

The goal in this work was to answer two independent questions.

First, we asked whether mesenchymal stem cells (MSC) were present in ear tissue of both species and compared their differentiation capabilities in vitro. Primary cell cultures were established from uninjured ears of both species, immune-phenotyped and cultured in vitro in adipocyte, chondrocyte and osteocyte differentiation media. Differentiation was characterized by staining and marker expression. We found that *Mus* cells tend to differentiate to adipocytes, while *Acomys* cells tend to differentiate to chondrocytes.

Second, we asked whether telomerase was differentially upregulated in *Acomys* vs *Mus* in response to wounding. Both species were subjected to ear wounds and allowed to heal or regenerate. Tissues were harvested at different time points and analyzed for TERT expression by RT-qPCR. Our results were inconclusive.

This work constitutes a further step in understanding the molecular and cellular mechanisms that distinguish *Acomys* as an emerging mammalian regeneration model.

Keywords: wounding; regeneration; fibrotic scarring; mesenchymal stem cells; telomerase; adipogenesis; chondrogenesis.

Resumo

Os organismos de todo o Metazoa diferem entre si em relação à resposta a ferimentos. As duas respostas base são regeneração ou fibrose. Enquanto grupos como axolotle, anfíbios e peixe demonstram capacidade regenerativa, mamíferos tendem a responder a ferimentos por fibrose.

Foi demonstrado que o Rato Espinhoso Africano (*Acomys*) fecha ferimentos na orelha com diâmetro de 4 mm, com completa regeneração da arquitectura original do tecido, incluindo derme, epiderme, cartilagem e folículos pilosos. Em contraste, o murganho (*Mus Musuculus*) apenas é capaz de cicatrizar as fronteiras da ferida. Deste modo, o *Acomys* e o *Mus* constituem um bom sistema comparativo para o estudo de regeneração em mamíferos.

O objectivo deste trabalho foi de responder a duas questões independentes.

Primeiro, colocámos a questão se existiam células estaminais mesenquimatosas (MSC) na orelha de ambas as espécies, e comparamos o seu potencial de diferenciação *in vitro*. Culturas de células primárias foram estabelecidas a partir de orelhas de ambas as espécies, o fenótipo imunitário foi caracterizado e as células foram cultivadas em meios indutores de adipogênese, condrogêndese e osteogênese. O potencial de diferenciação foi caracterizado por marcação histológica e expressão de marcadores moleculares. Observamos que células de *Mus* têm tendência em diferenciar para adipócitos, enquanto em *Acomys* a tendência é diferenciar para condrócitos.

Em segundo lugar, colocámos a questão se a telomerase apresentava níveis de expressão diferentes entre *Acomys* e *Mus* após lesão experimental na orelha. Ambas as espécies foram sujeitas a ferimento experimental nas orelhas, e foi permitido o processo de regeneração ou cicatrização. Os tecidos foram recolhidos em diferentes pontos no tempo e a expressão de TERT foi feita por RT-qPCR. Os nossos resultados foram inconclusivos.

Este trabalho representa mais um passo na direcção de perceber os mecanismos moleculares e celulares que destinguem o *Acomys* como um potencial modelo de regeneração em mamíferos.

Palavras-Chave: ferimento; regeneração; fibrose; células estaminais mesenquimais; telomerase; adipogênese; condrogênese.

Index

Figure Index

Table Index

Abbreviations

AIM - Adipogenesis-Inducing Media

Amph B – Amphotericin B

cDNA – complementary Deoxyribonucleic Acid

CIM – Chondrogenesis-Inducing Media

DIM – Differentiation-Inducing Media

ddH_2O – Double Distilled Water

DMEM – Dulbecco's Modified Eagle Medium

DMEMc – Complete Dulbecco's Modified Eagle Medium

DNA – Deoxyribunucleic Acid

FBS – Fetal Bovine Serum

FP – Forward Primer

gDNA – genomic Deoxyribonucleinc Acid

IBMX – 3-isobutyl-1-methylxantine

MB H_2O – Molecular Biology Grade water

MSC – Mesenchymal Stem Cell

PBS – Phosphate Buffer Saline

OIM – Osteogenesis-Inducing Media

PCR – Polymerase Chain Reaction

MRL – Murphy Roths Large

P/S (Pen/Strep) – Penicillin/Streptomycin

PFA – Paraformaldehyde

RT-qPCR – Reverse Transcription Quantitative Polymerase Chain Reaction

RNA – Ribonucleic Acid

RP – Reverse Primer

ON – Overnight

RT – Room Temperature

NTC – No template Control

NRT – No reverse transcriptase

RT (+) –Reverse Transcriptase Present

RT (-) – Reverse Transcriptase Absent

TERT – Telomerase Reverse Transcriptase

CD105 – Endoglin

CD45 – Protein tyrosine phosphatase, receptor type, c

CD29 – Integrin β-1

Sca-1 – Stem cells antigen-1

Chapter 1.

General Introduction to Regeneration and the *Acomys cahirinus* Model

1.1 Regenerative Mechanisms and Animal Models of Regeneration

In response to injury, a complex array of intracellular and intercellular pathways are activated and coordinated in order to re-establish tissue integrity and homeostasis. Most commonly, the response to injury across the Metazoa is through wound repair, which results in formation of a fibrotic scar.

However, some organisms across the Metazoa display some degree of regenerative responses to injury or trauma. Among the most robust regenerative systems are the Urodele amphibians (axolotls, salamanders), which are capable of complete limb regeneration. Newts and axolotls are also capable of regenerating brain, spinal cord and heart tissue (Brockes, 2002; Suzuki, 2006; McCusker, 2014).

Regeneration proceeds through three classical mechanisms: epimorphic regeneration, morphollaxis and compensatory regeneration (Brockes, 2002; Suzuki, 2006; McCusker, 2014). Epimorphic regeneration involves the dedifferentiation of adult cells proliferate to form a mass of undifferentiated cells. Subsequently, these cells differentiate, migrate and pattern themselves to give rise to the missing organ or tissue, without drastic rearrangement of the structures surrounding the wound bed. This type of regeneration is characteristic of regenerating limbs in species such as froglets of *Xenopus laevi* (Gilbert SF, 2000; Suzuki, 2006) and *Ambystoma mexicanum* (axolotl) (Seifert et al, 2012). The second mechanism (morphollaxis) is a response to injury consisting of the re-patterning of existing tissues (with little proliferation) to give rise to the missing structure. This type of regeneration is well characterized in the Hydra system, where it is thought to be due to the high degree of plasticity of differentiated Hydra cells (Koizumi et al, 1991; Gilbert SF, 2000; Agata et al, 2007). The third mechanism is known as compensatory regeneration. The best example of this mechanism is the regeneration of adult liver, where differentiated cells enter the cell cycle without de-differentiating, resulting in new cells assuming the functions of lost cells. This process usually occurs in normal physiological conditions, where loss of structures is not a result of injury, but rather a process of tissue self-renewal so that tissue functions are maintained (Chuong et al, 2012).

Contrary to amphibians, mammals are more limited in their capacity for limb and organ regeneration, and tend to respond to injury with fibrotic scarring. However, there are instances of homeostatic mechanisms mediated by regeneration. Tissues such as blood, skin and bone can continuously regenerate due to the existence of pools of multipotent stem cells. In adult humans, liver has an impressive capacity or regeneration, being capable of regenerating up to 70% of its mass after injury, which is achieved through hepatocyte hyperplasia (Miyaoka et al 2013). Another instance of regeneration is observable for early fetuses of different species, namely human, where skin regeneration proceeds in a way that results in repaired tissue devoid of scars. This capacity, however, is lost at later stages of development, with wounds resulting in fibrotic scar tissue (Rolfe et al, 2012; Satish et al, 2010).

In order to dissect the pathways and mechanisms underlying regeneration, there is the need for good model organisms that display robust and reproducible regenerative phenotypes. Current animal models in the field of regeneration include axolotls (*Ambystoma mexicanum*), the zebrafish (*Danio rerio*), African clawed frog (*Xenopus laevis)* and the planaria (*Schmidtea mediterranea*). However, regenerative phenotypes in mammals are uncommon and few models exist, such as ear closure in the MRL strain of mice (Edwards, 2008) and rabbits (Eslaminejad et al, 2013; Mahmoudi et al, 2011), digit tip regeneration in mice (Simkin et al, 2015) and the annual regrowth of deer antlers (Kierdof, 2012). One recent and remarkable addition to this list is the African Spiny Mouse, discussed in the following section.

1.2 The African Spiny Mouse (*Acomys cahirinus*)

The term ‘African Spiny Mouse’ is a collective reference to the genus *Acomys*, which owes its etymology to the spiny hairs that emerge from their dorsum. According to the International Union for the Conservation of Nature, there are currently 18 known *Acomys* species, habiting arid environments across Africa, the Middle East and Southern of Asia. They are larger than the common laboratory mouse, *Mus musculus*, with adults typically weighing between 40 and 50 g. One of their most notable characteristics is their precocial nature (Supplementary Figure 1). Newborn pups are born in an advanced stage of development compared to other murid rodents, with a full coat of soft grey hair, opened eyes and ears unfolded. Remarkably, they are capable of

locomotion and thermoregulation. *Acomys* have been used for studies of diabetes, perinatal research and more recently, regeneration.

Acomys have been used as a model of nutrition induced diabetes mellitus type II. Whilst on a high-energy diet, *Acomys* respond with obesity, low insulin levels and β-cell hyperplasia (Shafrir, 2006).

Due to their long gestation period (39 days) and precocity, *Acomys* develop most organ systems *in utero,* such as liver and kidneys (Dickinson et al, 2005), in contrast to altricial rodent pups, making them good models for perinatal research (Lamers, 1985; Dickinson, 2005). As such, spiny mice have been used to study the effect of maternal exposure to glucocorticoids, which have deleterious effects on placental function (Iwaniak et al, 2015). More interestingly, they have been used in studies to understand brain development *in utero* and the neural pathways of behavior (Brunjes et al, 1989).

More recently, two species of spiny mice, *Acomys percivali* and *Acomys kempi*, were shown to have a high degree of regenerative capacity. Both species show autotomy, a phenomenon by which dorsal skin and tail sheath were easily lost when mice were manipulated, possibly owing to the weak tensile strength of the tissues involved, presumably an antipredator adaptation. Animals can suffer large full thickness wounds, which, remarkably, heal in 30 days. Importantly, histological analysis of the affected region showed that animals reconstituted the original tissue architecture, rather than respond with fibrotic scarring, as is the norm in mammals. Furthermore, 4 mm full thickness wounds in ear pinna fully closed within 60 days, displaying the same level of robust regeneration as seen for the skin (Seifert et al, 2012).

In our group, we have shown that the regenerative phenotype extends to a third member of the genus (*Acomys cahirinus)*. Four-millimeter full thickness wound in the ear pinna showed complete regeneration of tissue architecture, including dermis, epidermis, sebaceous glands, adipose tissue hair follicles, angiogenesis and nerve fiber regeneration (Figure 1). *Mus*cle fibers were also found in the regenerated region (Santos et al, 2016). A side-by-side comparison of 4-mm full thickness ear pinna wounds in *Acomys* and *Mus* resulted in the *Acomys* ear wound full closure within 60 days, in contrast to *Mus,* which merely healed the borders of the wound through fibrotic scarring with no significant wound closure.

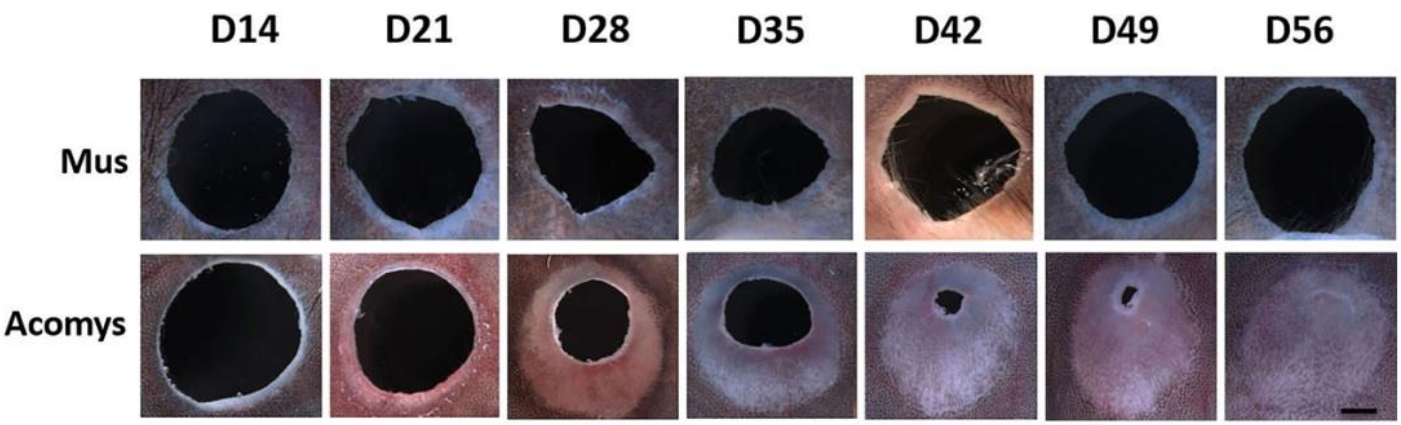

Figure 1. Ear Hole Closure Timeline for *A. cahirinus* vs. *Mus musculus*: response to 4 mm full thickness ear wounds at weekly intervals between day 14 and 56 (220x, scale bar 1 mm; distal-proximal axis shown vertically with distal at top and proximal at bottom for all panels) (Santos et al, 2016).

The work performed in this thesis sought to address two independent questions:

1) Given the ability of MSC to differentiate to multiple cell types, are mesenchymal stem cells (MSC) present in the ear of *Acomys cahirinus* and if so, can the different responses of *Acomys* vs. *Mus* to ear pinna wounding be explained by difference of the behavior of MSC in both species?

2) Given the role of telomerase in certain regenerating systems sucha as zebrafish, does the regenerative response to ear pinna wounding observed in *Acomys cahirinus* involve upregulation of the telomere extending machinery in regenerating tissues?

1.3 Bibliographical References

Brunjes C. P., Korol D. L., Stern K. G., "**Prenatal neurogenesis in the telencephalon of the preocial mouse *Acomys cahirinus***", *Neuroscience Letters*, (1989), 107, pp. 1-3

Chuong CM., Randall V. R., Widelitz R. B., Wu P. Jiang TX., "**Physiological regeneration of skin appendages and implications for regenerative medicine**", *Physiology (Bethesda)*, (2013), 27(2) pp. 61-72

Gilbert SF. Developmental Biology. 6th edition. Sunderland (MA): Sinauer Associates; 2000. Regeneration. Available from: https://www.ncbi.nlm.nih.gov/books/NBK9971/

Gonzalez A., Costa T., Andrade Z., Medrado A., "**Wound Healing – A literature review**", *An Bras Dermatol* (2016), 91(5), 614-620

Gurtner G C., Werner S., Barrandon Y., Longaker M. T., "**Wound Repair and Regeneration**", *Nature* (2008), Vol. 453, 314-321

Iwaniak P., Dobrowolski P., Tomaszewska E., Hulas-Stasiak M., Tomcyk A., Gawron A., "**The influence of dexamethasone administered prenatally on cartilage of newborn spiny mouse (*Acomys cahirinus*) offspring**", *J Dev Orig Health Dis*, (2015), 17, pp 1-8

Lamers W. H., Mooren P. G., Graaf A. D., Charles R., "**Perinatal development of the liver in rat and spiny mouse Its relation to altricial and precocial timing of birth**", *Eur. J. Biochem.*, 146, 475-480 (1985)

Miyaoka Y., Miyajima A., "**To divide or not to divide: revisiting liver regeneration**". *Cell division* 8: 8

Shaw T J., Martin P., "**Wound Repair at a Glance**", *Journal of Cell Science* (2009), 122, pp. 3209-321

Chapter 2.

In vitro Ear Cell Differentiation Capacity of *Acomys cahirinus* vs. *Mus musculus*

2.1 Introduction

Among adult stem cells, mesenchymal stem cells (MSCs) are multipotent stem cells that can differentiate into various cell types, such as adipocytes, osteoblasts, chondrocytes, myocytes, β-pancreatic islets cells, and potentially, neural cells (Nombela-Arrieta, 2011, Gao, 2016). In addition, recent *in vivo* studies have demonstrated their capacity for self-renewal. They can be cultured *in vitro*, show adherence to polystyrene surfaces, have low immunogenicity and can be regulators of the immune response. MSCs have been reported to be capable to suppress the activation and function of cells from the innate (such as macrophages, neutrophils and dendritic cells) and adaptive systems (T lymphocytes and B-lymphocytes). This is due to an arrest of the immune cells in G0/G1, thus preventing entry in the cell cycle. Furthermore, concrete mechanisms, such as the inhibition of proliferation of B lymphocytes by IFN-γ-treated MSCs have helped to understand the interactions that MSCs have with the immune system, information that could prove valuable in the field of regenerative medicine (Mundra et al 2013; Kolluri et al 2013; Wang et al 2014).

The International Society of Cellular Therapy (ISCT) has defined minimal criteria for mesenchymal stem cells (Horwitz et al., 2005). According to these criteria, MSCs *Mus*t:

- Adhere and grow in a plastic substrate when cultured *in vitro*;
- Be capable of multilineage differentiation to adipocytes, chondrocytes and osteoblasts when subjected to Differentiation Inducing Media (DIM);
- Express a specific panel of surface markers. In humans, MSCs are positive for CD73, CD90 and CD105 surface antigens, while lacking CD34 and CD45 leukocyte markers. In mouse, MSC are positive for CD105, CD29 and Sca-1, while being negative for CD45.

The first to isolate and describe MSC cells was Friedenstein, who described the isolation of spindle-shaped, clonogenic cells from bone marrow which he initially defined as colony-forming unit fibroblasts (Uccelli et. al. 2008). After the characterization of these cells regarding their

capacity of self-renewal and tri-lineage differentiation the term Mesenchymal Stem Cells started to be used to refer to these precursor cells.

Although initial reports focused solely on bone marrow-derived MSCs, further reports have demonstrated that MSCs can be derived from other tissues such as adipose, umbilical cord, cord blood, dental pulp and the amniotic membrane (Rohban et al 2017). Furthermore, depending on the tissue of origin, MSCs have shown differential regenerative capabilities. Bone marrow derived MSCs possess a higher potential to give rise to chondrocytes and osteoblasts when compared to MSCs derived from adipose tissue, who have a higher tendency for capillary formation and vasculogenesis *in vivo*. The variability and extent in regenerative potential of MSC populations are still unknown, but it is believed that stem cell niche influence over cell fate, genetic variability and/or epigenetic factors are major contributors to the differences seen between MSCs derived from different tissues (Rohban et al 2017).

Since their discovery, MSCs applications and possible translation into clinical therapies has steadily risen. According to Squillaro et al. 2016, the number of MSC-based clinical trials as nearly doubled in the past three years, pointing to the potential of MSC-based therapeutics in cases of injury or disease.

Interest in MSCs was initially focused on their application on cellular therapies, but research has indicated that the potential of MSCs for other applications is due in great part to their immunosuppression capability and lack of immunogenicity (Mundra et al, 2013; Wang et al, 2014). MSCs do not express the class II major histocompatibility complex (MHC) on their cell surface, nor do they present the classical co-stimulatory molecules, such as CD80, CD86, and CD40, thus making them prime candidates for allogenic transplantation (Mundra et al, 2013)

The reduced immunogenicity and the tropism of MSC towards wound beds and regions of new stroma formation are also of interest for delivery system therapies. MSCs have used as vectors for delivery of therapeutic compounds, such as pro-apoptotic agents into tumor micro-environment (Kolluri et al 2013), or in gene therapy applications (Mundra et al 2013).

MSC have also been reported to have clinical application in the treatment of immune-mediated diseases, such as Type 1 Diabetes. Murine MSC delay the onset of diabetes development when transplanted into diabetes prone mice prone (Fiorina et al. 2009). Given their plasticity, MSCs

have been transdifferentiated into functional pancreatic β-cells, which could improve the current therapeutic approaches for type 1 diabetes. This transdifferentiation of MSC to insulin producing cells can be achieved by reprogramming MSCs with adenoviruses expressing pancreatic specific transcription factors (Mundra et al, 2013). It is also possible to induce differentiation of MSCs into a pancreatic endocrine phenotype by manipulating the culture conditions (Santos et al, 2010)

In the field of regenerative medicine, MSCs have been employed in clinical trials with the goal of regeneration of tissues, such as bone and cartilage, the treatment of disorder such as spinal cord injury, Crohn's disease and graft-versus-host disease. The coculture of MSC with endothelial colony forming cells resulted in the formation of stable and perfused microvessels, pointing out to a potential role of MSCs in neovasculogenesis (Rohban et al, 2017). In other reports, MSCs served as pericytes, wrapping around blood vessels and offering support to their structure and stability.

In our lab, we are interested in understanding whether MSC play a role in the robust regenerative response of *Acomys cahirinus*. Ear MSCs could proliferate and migrate to the wound bed, undergo differentiation to one or more cell types present in the regenerated tissue, or have an immunoregulatory effect. Differences in the MSC compartment might partially explain the different responses to ear punch injury in *Acomys cahirinus* and *Mus musculus.*

We therefore attempted to identify MSC in the ear tissue of *Acomys* and *Mus*. To do so, we harvested cells for these tissues, immunophenotyped them and analyzed their *in vitro* differentiation capacity.

2.2 Materials and Methods

2.2.1 Husbandry and handling of *Acomys cahirinus*

All procedures in laboratory animals were done in accordance with the guidelines by the Sociedade Portuguesa de Ciência em Animais de Laboratório (SPCAL). All animals selected for experimentation were at approximately 2 months of age for both species.

Laboratory animals were kept in plastic cages. Room temperature was kept at 25ºC, with automated light-dark cycles of 12 hours of light and 12 hours of dark. Animals were fed with a high protein and fiber diet and fresh fruit, with *ad libitum* access to bottled water.

Handling of animals was done with proper hand protection. Animals to be subjected to experimentation were anesthetized with isofluorane (Abbott, IsoFlo). Animals were closely observed for signs of anesthesia, such as inaction, decrease of respiratory rate, lack of response to external stimuli, relaxation of tail, etc. Animals were placed on a clean warm surface, to prevent sources of infection and rapid decrease of body temperature leading to hypothermia. Before starting any procedure, tail and paw pinch were performed to confirm the animal was under a deep state of anesthesia and there was no pain and/or discomfort for the animal.

All surgery material used was previously sterilized. Post experimentation, animals were placed in clean cages with fresh bedding in order to decrease sources of infection and to help recovery.

2.2.2 Tissue Harvesting and Ear Cell Culture Establishment

Ears were excised with sterile scissors and placed in 70% Et-OH for 30 seconds, in order to clean the tissue surface of possible sources of contamination before proceeding for *in vitro* procedures. Ears were then submerged in cold 1X PBS + 2X P/S (Gibco) + 2X Amph β (Gibco, Cat No. 15290018) in a 50 ml Falcon tube (Sarstedt, 62.547.254) and kept on ice for transportation to the Tissue Culture Unit; transportation time was under 5 minutes.

Samples were placed on a petri dish on top of ice and sectioned into small pieces with a surgical blade. The resulting “pulp” was transferred into a 15 ml Falcon tube (Sarstedt, 62.554.502). Depending on the tissue volume, 1 to 5 mL of 0.25% Trypsin (Gibco) was added, and the sample incubated at 37ºC. After 15 minutes, the suspension was centrifuged at 1000 RPM for 2 minutes, supernatant was taken and passed by a 70 µm strainer (VWR, 21008-952) to a 50 ml Falcon tube and at least double the volume of warm culture media (DMEM+ 1X GlutaMAX + 20% FBS + 2X P/S + 2X Amph) was added. After passage of the suspension through the strainer, 2 ml of 0.25% Trypsin was added to the digested tissue pellet that remained at the bottom of the first Falcon tube, and again placed in a water bath for 15 minutes, after which the procedure was repeated until all tissue was digested. From the resulting cell suspension, an aliquot of 10 µl was

taken and placed on a Neubauer chamber for cell counting. Given that the flow cytometry protocol (detailed further down) set the minimum concentration of $1x10^6$ cells per ml of media, if concentration was too low, cell suspension was centrifuged at 1000 RPM for 5 minutes, the supernatant removed and the cell pellet resuspended in an adequate amount of media. The resulting cell suspension was fractioned, with one fraction being seeded unto 10-cm polystyrene culture dishes (Sarstedt), and incubated at 37ºC and 5% CO_2 for expansion while the second fraction was subjected to flow cytometry analysis.

2.2.3 Flow Cytometry Analysis

Flow cytometry analysis was performed on two cell populations: cells directly harvested from the ear tissue and not yet seeded unto a polystyrene surface (P0), and to the resulting cell population after *in vitro* expansion up to the point of confluency (P1). Flow cytometry analysis was performed for both *Mus musculus* and *Acomys cahirinus* cells using the same Multi-Color Flow cytometry kit (FCK) (R&D Systems, FMC003). Cells were washed in 5 ml of pre-warmed 1X PBS, centrifuged at 1000 RPM during 5 minutes, and the cell pellet resuspended to a final concentration of 1 million cells per ml in FCK resuspension buffer. Aliquots of 1 million cells of the resulting cell suspension were transferred to cytometry tubes and 10 µl of an individual antibody (CD105, CD29, Sca1 and CD45 respectively) added. Additionally, a tube with no addition of antibody (negative control) and addition of all four antibodies were set up.

Samples where then incubated for 45 minutes at room temperature protected from light. After the incubation period, the tubes were centrifuged at 1000 RPM for 5 minutes, supernatant was removed and 1X PBS was added. Tubes proceeded for flow cytometry analysis and data analyzed with Infinicyt™ software.

2.2.4 Differentiation Inducing Media

All culture media described were prepared in sterile conditions and filtered through a 0.22 µm filter. The media compositions were as follows:

Adipogenesis Induction Medium (AIM) (Baghaban-Eslaminejad, 2013)

- DMEM + 10% FBS + 1X P/S + 1X Glutamax

- 100 nM dexamethasone (Sigma-Aldrich, D4902)
- 50 µg/ml indomethacin (Sigma-Aldrich, I7378)
- 500 µM IBMX (TORIS Bioscience, 2845)
- 10 µg/ml insulin (Sigma-Aldrich, I2643 1001561376)

Chondrogenesis Induction Medium (CIM) (Newman, 2001)

- DMEM/Hams' F12 + Glutamax (1:1) (Sigma-Aldrich, 10565-018) + 5% FBS + 1X P/S
- 10 µg·ml-1 insulin (Sigma-Aldrich, I2643 1001561376)
- 10 µg·ml-1 transferin (Sigma-Aldrich, T8158 101316524)
- 30 nM sodium selenite (Sigma-Aldrich, S5261 1001543979)

Osteogenesis Induction Medium (OIM) (Herlofsen, 2011)

- DMEM + 20% FBS + 1X P/S + 1X Glutamax
- 50 µg·ml-1 sodium ascorbate (Sigma Aldrich, A7631)
- 10 nM dexamethasone
- 10 mM β-glicerophosphate (Sigma-Aldrich, G9422)

2.2.5 Cell Culture Staining Procedure

Prior to staining, cell cultures were washed with pre-warmed 1X PBS, fixed with 1X PBS 4% PFA (Sigma-Aldrich, P6148) overnight at 4C, changed to cold 1X PBS and stored at 4ºC until staining.

Oil Red O staining

A stock solution was prepared by dissolving 60 mg of Oil Red O powder (Sigma-Aldrich, O0625), in 20 ml isopropanol, and left rocking for at least 20 minutes. This solution is stable for 1 year. Working solution was prepared by mixing 3 volumes of the stock solution with 2 volumes of ddH_2O, and filtered through a Whatman paper to eliminate non-dissolved solids. Oil Red O working solution was added to the cell culture and left for 20 minutes at RT with gentle rocking. Samples were then washed with ddH_2O two times and observed under the optical microscope.

Alcian Blue Staining

A working solution of 0.5% (w/v) Alcian Blue 8GX (Sigma-Aldrich, A5268) in 0.1 N hydrochloric acid (Sigma-Aldrich, 258148) was prepared and filtered through a Whatman paper. Cell cultures were stained overnight at 4ºC with gentle rocking. Samples were then washed with ddH_2O two times and observed under the microscope.

Alizarin Red Staining

A working solution of 40 mM Alizarin Red was prepared by dissolving 274 mg of Alizarin Red powder (Sigma-Aldrich A5533) in 19 mL of ddH_2O. pH was adjusted to 4.2 with 1% ammonium hydroxide, ddH_2O was then added to a final volume of 20 ml and the solution was filtered through a Whatman paper. Samples were stained for 5 minutes and washed two times with ddH_2O before observation under the microscope.

2.2.6 RNA Extraction

Total RNA from frozen cell pellets was extracted using the Zymo Research *Quick-RNA*™ MiniPrep kit (Zymo Research, R1054).

2.2.7 RT-qPCR Assay and Procedure

Total RNA (1 ug) was reverse transcribed (resulting in a RT+ cDNA fraction) using an iScript cDNA Synthesis Kit (Bio-Rad, 170-8891), following the manufacturer's instructions. A control reaction was set up without reverse transcriptase (RT- cDNA fraction). Reactions were conducted in a C1000 Touch Thermal Cycler (Bio-Rad).

qPCR was performed using SSoFast EvaGreen Supermix (Bio-Rad, 172-5201) in a 96 well plate format on a CFX96 Real-Time PCR System (Bio-Rad).

2.3 Results and Discussion

2.3.1 Establishment of Ear Cell Primary Cultures

The protocol that was described in Materials and Methods was the result of successive optimizations.

In an initial protocol (previously developed in our lab), 2 animals were anesthetized with isofluorane, both ears were harvested and submerged 30 seconds in 70% ethanol and then transferred to cold 1X PBS supplemented with 2X Amph B, on ice. Transport of the samples to the tissue culture unit took less than 5 minutes. While inside the laminar flow hood, ears were cut into smaller pieces with the aid of a sterile scalpel, and once a pulp was obtained, the tissue was transferred to a 15ml Falcon tube. 1X PBS was then added to a final volume of 15 ml to wash the tissue. The suspension was centrifuged for 5 min at 1000 RPM, and the supernatant was discarded. 0.25% trypsin was added, and the tissue was incubated at 37ºC for 1h. Samples were mixed by inversion every 20 minutes. Pre-warmed DMEMc (DMEM + 20% FBS + 2X P/S + 1X Glutamax + 1X Amph B) was added to a final volume of 15 ml. The mixture was passed through a 70 µm strainer, and the resulting suspension was plated onto a 10 cm polystyrene culture dish for culture at 37ºC and 5% CO_2.

The culture dishes were left untouched for a minimal period of 48 hours, and then observed under the microscope. Although the cellular output for this protocol was high, there were also high levels of cellular debris and very low cell adherence. Surviving cells did not reach confluence before exhibiting a senescent phenotype. In an attempt to improve cell viability, we decided to optimize the time of digestion and the concentration of trypsin.

Time of digestion

We reasoned that during the 1 hour digestion period of the initial protocol, cells that separated from tissue early during the digestion would be exposed to trypsin for much longer than those cells being digested out of the tissue late during the digestion, perhaps explaining the low viability. We adjusted total time of digestion and the period between sample shaking, while keeping all other parameters equal.

In a first experiment consisted in a reduction of the digestion time to 30 minutes, with shaking of the sample every 10 minutes. We observed a higher degree of cell adherence and cell division, but we obtained lower cell yield due to incomplete digestion of ear tissue.

In a second experiment, we extended the total time of digestion back to 1 hour, and digestion was done in two parts of 30 minutes. Tissue would be digested during 30 minutes with shaking every 10 minutes. After 30 minutes, sample was centrifuged at 1000 RPM for 2 minutes. Supernatant was then passed through a 70 µm strainer, and at least double the volume of DMEMc was added. The undigested tissue remaining was subjected to another 30 minutes of digestion with fresh trypsin. Both suspensions of single cells were pooled. This procedure resulted in a reduction of the debris in cell cultures, but no significant improvement in cell adherence and proliferation.

Concentration of Trypsin

To optimize trypsin concentration, two experiments were performed:

1. In a first experiment, trypsin concentration was reduced to 0.05%, while all other parameters were kept constant. We observed less single cells in suspension, and an increase in cell aggregates and cellular debris.
2. In a second experiment, we added a 30 minute incubation period on ice after adding 0.25% trypsin to allow for a better permeation of the tissue by the enzyme before transferring to the optimal temperature of digestion (37ºC). We did not observe any improvement compared to the standard protocol.

We then designed and tested the procedure described in Materials and Methods (starting from a total of 4 animals). By using 0.25% trypsin for 4 consecutive periods of digestion at 37ºC for periods of 15 minutes and harvesting 4 fractions of cells (one at the end of each incubation period) we obtained a yield of pooled cells that, when plated on a 10 cm dish demonstrated reasonable plating efficiency and growth, with *Acomys* cells reaching confluency in between 13 to 15 days, and *Mus* cells in between 2-3 weeks.

2.3.2 *In vitro* Differentiation of Ear cell primary cultures

Primary cultures typically yielded a heterogenous population of cells. Although ears of both species were processed in the same way, we cannot affirm that the resulting cell population were

equivalent in identity or characteristics. In particular, we were interested in determining what percentage of cells isolated by our procedure were MSC.

2.3.3 Identification of MSC by Flow cytometry

We characterized the cells for their cell surface markers with a multi-color flow cytometry assay, to determine if the initial cell populations that were seeded on the culture dish, passage 0 (P0), and the cells that were split after expansion, passage 1 (P1) showed any differences in cell types and proportions.

Results are summarized in **Table 1.** In *Mus*, 10.21% of the P0 population had a MSC immune-phenotype. Further, 39.87% of the cells were CD29+ CD105- Sca1+ CD45-, i.e. had what could be called an MSC-like immune-phenotype (lacking only CD105). After a period of proliferation (at P1), the MSC population (CD29+ CD105+ Sca1+ CD45-) was reduced to 5.27% of the population while the MSC-like population (CD29+ CD105- Sca1+ CD45-) remained at similar levels (39.82%). Given that MSC in mouse ear tissue have not been previously characterized, we speculated that the population lacking CD105 might still behave as MSC in terms of their differentiation potential.

Surface Markers	***Mus* (Passage 0)**	***Mus* Passage 1)**	***Acomys* (Passage 0)**
Other Events	16.74	20.01	6.11
No Markers	0.87	2.08	73.48
CD105 + only	0.01	0.01	1.9
CD29+ only	0.55	0.83	9.23
Sca1+ only	2.25	5.65	4.39
CD45+ only	0.17	0.13	0.27
CD29+ CD105+ Sca1- CD45-	0.03	0	1.4
CD29- CD105+ Sca1+ CD45-	0.03	0.04	0.14
CD29- CD105+ Sca1- CD45+	0	0	0.42

CD29+ CD105- Sca1+ CD45-	39.87	39.82	0.84
CD29+ CD105- Sca1- CD45+	0.5	0.66	0.17
CD29- CD105- Sca1+ CD45+	0.41	0.39	0.04
CD29+ CD105+ Sca1- CD45+	0.21	0.19	0.22
CD29- CD105+ Sca1+ CD45+	0.01	0.03	0.09
CD29+ CD105- Sca1+ CD45+	17.04	16.85	0.04
CD29+ CD105+ Sca1+ CD45-	10.21	5.27	0.96
CD29+ CD105+ Sca1+ CD45+	11.11	8.03	0.3

Table 1. Relative proportions of cell populations in percentage for all possible combinations of surface marker antigens. The first column displays the percentages of a surface marker or combination of surface markers for ear cells of *Mus musculus* after processing but before seeding on to a culture dish, and the second column the percentages for these cell populations after seeding and expansion. The third row displays the percentage results for ear cells *Acomys cahirinus* after processing but before seeing on to a culture dish.

In *Acomys*, we observed strikingly low levels of cells bearing the markers tested in practically all possible combinations. Given that the percentage of cells showing the MSC immunophenoptype was 0.96%, it was not considered worthwhile to test cells at P1. There are three possible reasons for these low numbers.

One possibility is that *Acomys* ears do not have MSC bearing the typical immune-phenotype to begin with. The second possibility is that the mouse specific antibodies used do not cross-react with *Acomys* and therefore do not label MSC. However, we found 9.23% and 4.39% of cells labeled only for CD29 or Sca1, suggesting that these antibodies do cross-react with *Acomys* epitopes (although cross-reaction with a different epitope cannot be ruled out). Even if one assumes that these antibodies recognize their intended epitopes, the number of cells with a CD29+ Sca1+ phenotype is 0.84%. A third possibility is that *Acomys* ears do contain cells with

MSC-like differentiation capabilities, but their cell surface markers are different from those found in mouse MSC.

Therefore, our results suggest that *Mus* ears contain relatively low numbers of MSC but were inconclusive for *Acomys*.

2.3.4 Multi-Lineage Differentiation of Adult Ear Primary Cultures

Regardless of the immunophenotyped profiles found in our cultures, we set out to test the differentiation potential of cells present in the ear of *Acomys*, in comparison to *Mus*. P1 cells of both species were passaged on to 60 cm polystyrene culture dishes ($1.5x10^5$ cells per dish) in DMEMc media and incubated at 37ºC and 5% CO_2 for a period of 24 hours. Once cells had attached to the substrate, the media was carefully removed, and specific differentiation media for adipocyte, chondrocyte and osteocyte differentiation was added to the plates. One set of plates were maintained in DMEMc as a non-differentiation control.

To test the differentiation potential of cells of a given species (*Acomys* vs. *Mus*) for a given fate (adipogenic, chondrogenic or osteogenic), or in DMEMc (as a non-differentiation medium control), cells were cultured for 5 weeks. Culture media was changed every 3 days. Cultures were set up in duplicate, with one complete set reserved to perform staining for adipocytes, chondrocytes or osteocytes. The second set was reserved for RNA extraction in order to view differences in the genetic expression of differentiation markers. Cultures were harvested at 7, 14, 21, 28 and 35 days after differentiation media was added to the plates. During this time, cell cultures were observed daily in order to check for contamination, monitor possible pH changes due to media exhaustion and observe any obvious morphological change in the population.

2.3.5 Analysis of Differentiation using Histological Stains

Cell differentiation throughout the time course of culture was assessed by morphology, by histological staining for specific cell types (adipocytes, chondrocytes and osteocytes). Histological stains were quantified by counting stained cells in representative regions of the culture.

Adipogenesis

A well established method to evaluate differentiation to adipocytes is Oil Red staining, which stains fat cell lipid deposits with an intense red coloring.

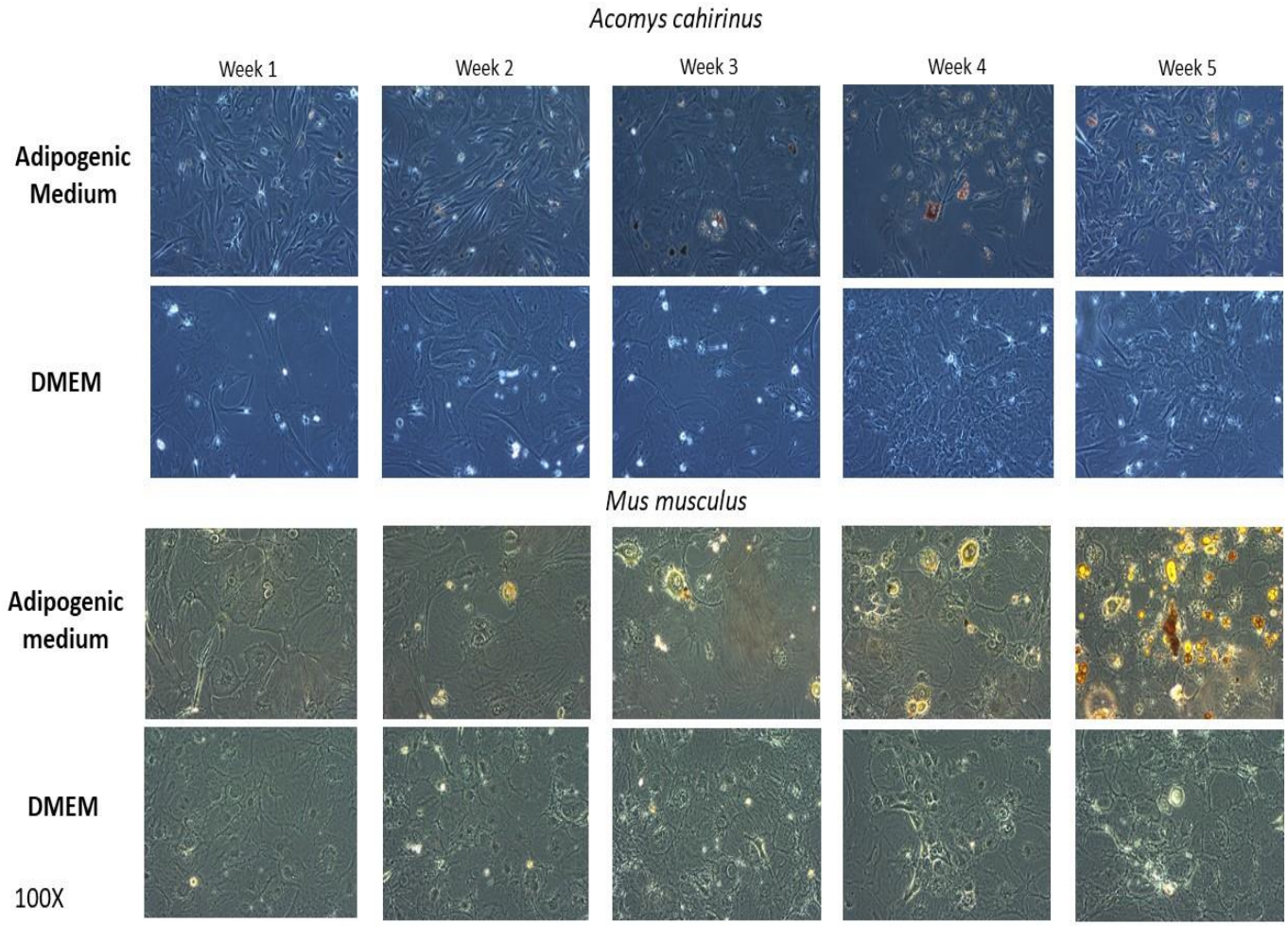

Figure 2. Comparison of adipogenesis in ear cells of *Acomys* vs *Mus*, from week 1 through week 5, cultured in AIM vs. DMEMc, (100x) and stained with Oil Red O.

Results are shown in Figure 2. Oil red staining shows a significantly greater propensity towards the adipocyte fate for *Mus* cells compared to *Acomys* cells, confirming preliminary results obtained previously in our lab (I. Casanellas). The difference was particularly noticeable at weeks 4 and 5. Cell cultured in DMEMc did not show staining.

Chondrogenesis

Cartilage is rich in polysaccharides such as glycosaminoglycans, which stain blue with Alcian Blue, a dye typically used to identify cartilaginous tissue.

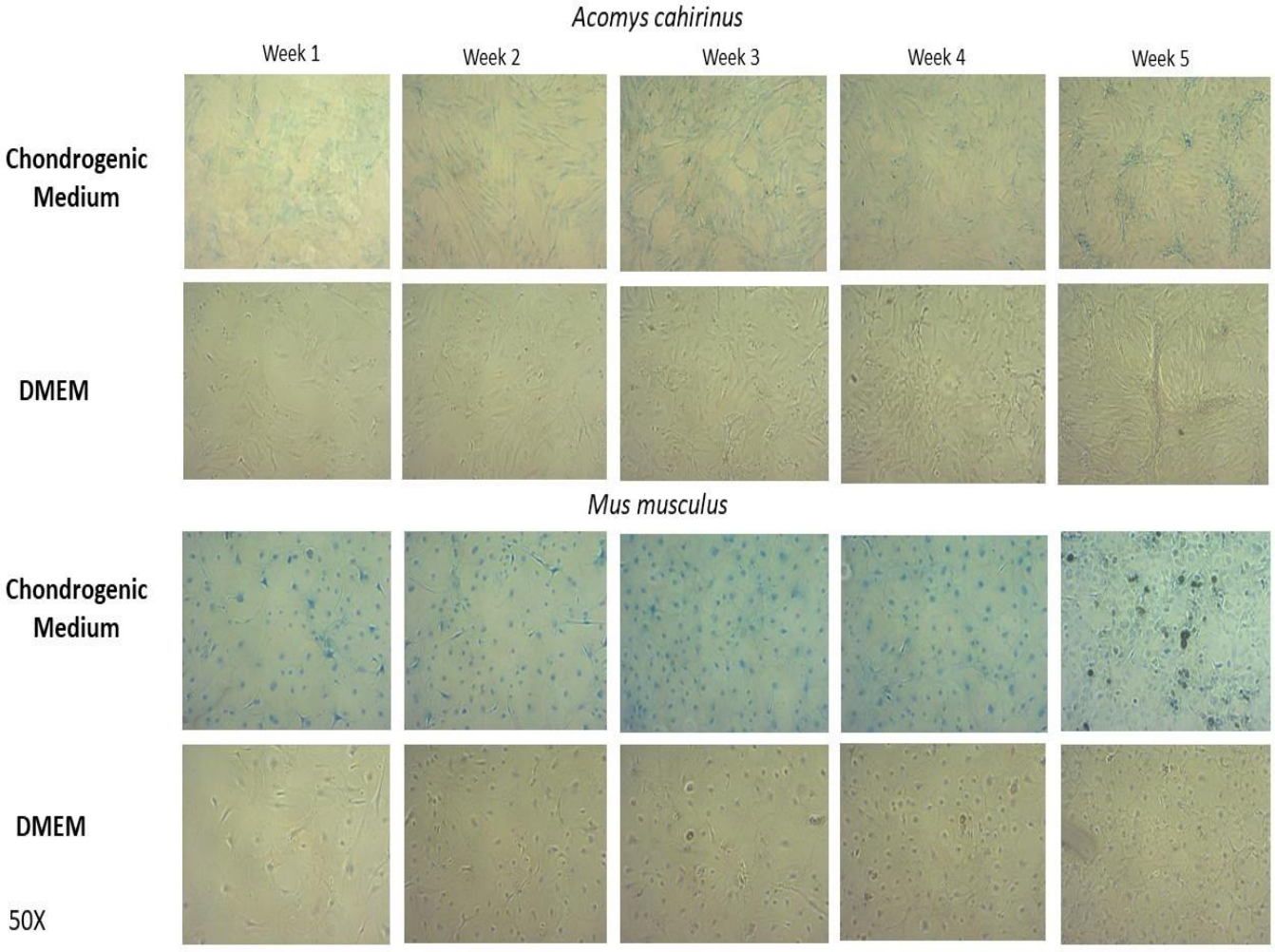

Figure 3. Comparison of chondrogenesis in ear cells of *Acomys* vs *Mus*, from week 1 until through week 5, cultured with in CIM vs. DMEMc, (100x) and stained with Alcian Blue.

Results are shown in Figure 3. *Mus* cell cultured in CIM seemed to show faint cytoplasmic blue stain at week 1, but the stain did not increase during culture up to week 5. To the contrary, *Acomys* cells cultured in CIM showed a faint level of patchy Alcian Blue staining which increased progressively up to week 5. *Mus* or *Acomys* cells cultured in DMEMc did not stain with Alcian Blue. We conclude that Alcian Blue staining suggests that *Acomys* ear cultures have a greater propensity to differentiate to the chondrocyte fate than *Mus* cells.

Osteogenesis

Primary ear cultures for both *Acomys* and *Mus* were cultured under osteogenic conditions and stained with Alizarin Red S to determine the degree of differentiation to the osteogenic fate over the time course of 5 weeks. However, we did not observe Alizarin Red staining or morphological differences between species or culture conditions, suggesting that osteogenic cells are not present in either species (data not shown).

In conclusion, staining of differentiated *Acomys* and *Mus* cells with Oil Red and Alcian Blue suggested that (at least) subpopulations contained in the culture of *Mus* are capable of adipogenic differentiation while subpopulations contained in the culture of *Acomys* are capable of chondrogenic differentiation.

2.3.6 Lineage Specific Marker Expression

Our initial observations using Oil Red and Alcian Blue stains suggested a that *Acomys* cultures contained a subpopulation capable of differentiating to the chondrogenic fate (while not such subpopulation was apparent in *Mus*), while *Mus* cultures seemed to contain a higher proportion (compared to *Acomys*) capable of differentiating to the adipogenic fate. We sought to confirm these differences by measuring expression of a number of marker genes specific for adipogenesis or chondrogenesis during our 5 weeks differentiation protocol. Candidate marker genes are listed in Table 3.

For all these genes, we designed primers that would amplify both *Mus* and *Acomys* genes. To do so we aligned cDNA sequences from *Mus* (available in Genebank) with cDNA sequences of

Acomys provided by a collaborator (Dr. A. Seifert, University of Kentucky, USA) and designed primers that met the following characteristics: a) bind to the sequence of both species (conserved binding sites); b) span exon-exon junctions to avoid amplifying any contaminating gDNA present in the reverse transcribed RNA sample; c) size between 18 and 22 nucleotides; d) amplify amplicons between 70 and 200 nucleotides; d) had similar annealing temperatures (approximately 60ºC); e) contained a G or a C in the 3' position and less than 3 Cs or Gs in the last most 3' bases; f) showed lack of significant self-complementarity to avoid hairpin formation; g) lacked significant complementarity between forward and reverse primers to avoid primer-dimer formation. All primers were designed with Primer3 software and are displayed in Table 2.

Reference Genes	
Target Gene	**Sequences**
GADPH PP1	FP: TGGCATTGTGGAAGGACTCA RP: CAGGGATGATGTTCTGGGCA
GADPH PP2	FP: GGCATGGCCTTCCGTGTT RP: CAGTGGGCCCTCAGATGC
Eif1α PP1	FP: GTGACATGTTAACACTTTGTGCT RP: CAGAACTGCTGACACAAAACAC
Eif1α PP2	FP: TGGTGTTTAAAGAGGATGGGCA RP: AATGTCCGAGGTATTTATCCAAAC
β-Actin PP1	FP: CCTGTGCTGCTCACCGAG RP: ATGGCTACGTACATGGCTGG
β-Actin PP2	FP: GGCTCCTAGCACCATGAAGA RP: CTGGAAGGTGGACAGTGAGG

Adipogenic	
Target Gene	**Sequences**
LPL PP1	FP: CAACCACAGCAGCAAGACC RP: CACCAGCTTGGTGTAGCCAG
LPL PP2	FP: CTGGCTACACCAAGCTGGTG RP: GTTAGGCCCAGCTGGATCC
LPL PP3	FP: CACGGAGGTGGACATCGGAG RP: CTTTCCCTTCTGCAGATGAG
Pparg PP1	FP: GTCAGTACTGTCGGTTTCAG RP: ATCAGCAGACTCTGGGTTCA
Pparg PP2	FP: GTCAGTACTGTCGGTTTCAG RP: TGGGTTCAGCTGGTCGATA
FABP4 PP1	FP: CACCATCCGGTCAGAGAGTAC RP: ACCACCAGCTTGTCACCATC
FABP4 PP2	FP: CACCATCCGGTCAGAGAGTAC RP: TGGTCGACTTTCCATCCCAC

Chondrogenic	
Target Gene	**Sequences**
Col2a1 PP1	FP: CTCCTGGTACTGATGGTCCC RP: CTCTCACCAGGCATTCCC
Sox9 PP1	FP: CTGCAAGCCGACTCCCC RP: GTTTTGGGAGTGGTGGGTGG
Runx3 PP1	FP: TCAGCAGCCAGGCCCA RP: CTCTGCAGCGTAGGGAAGGA

Adamts5 PP1	FP: GCAAATGGCAGCACCAA RP: CTGCCATTCCCAGGGTG

Table 2. Primer pairs designed for RT-qPCR (FP: forward primer; RP: reverse primer)

2.3.7 Validation of Primer Pairs

Care was taken to validate all primer pairs designed by determining their efficiency and specificity. This was done by testing primers pairs on tenfold serial dilutions of cDNA produced by reverse transcription of RNA extracted from tissues that are known to express the marker genes. Three to four primer pairs per gene were tested and only primer pairs with efficiencies between 90% and 110%, an R2 of 0.99 and a single melting curve peak were selected for use. Details of primer validation can be found in Appendix I.

The RNA used for cDNA synthesis for the validation of primer pairs had a RQI value of 7 or more for all instances. Primer pairs targeting reference genes were validated in both *Acomys* and *Mus* cDNA. Primers that target genes specific for the adipogenic lineage were tested using *Mus* cDNA, synthesized from RNA extracted from adipose tissue, and primers targeting genes specific for the chondrogenic lineage were tested using ATDC5 cell line Total RNA. The results are shown in Table 3.

Target Gene		**Efficiency (%)**	**Specific?**	**R^2**	**Slope (Cq/Log(SQ))**	**NRT and NTC**	**Usable?**
Reference Genes	**GADPH** PP2	96.2	Yes	0.999	3.415	Clear	Yes
	Eif1α PP1	97.4	Yes	0.996	3.385	Clear	Yes
	Actinβ PP1	109.1	Yes	0.998	3.124	Clear	Yes

Adipogenic Genes	**LPL** PP2	99.7	Yes	0.965	3.329	Clear	Yes
	PPARG PP1	158.1.0	Yes	0.880	2.071	Clear	No
	PPARG PP2	107.7	Yes	0.955	3.151	Clear	Yes
	FABP4 PP1	109.7	Yes	0.994	3.005	Clear	Yes
Chondrogenic Genes	**Sox9** PP1	338.5	Yes	0.626	1.558	Clear	No
	Sox9 PP2	98.9	No	0.308	0.513	Clear	No
	Col2α1 PP1	100,4	Yes	0.926	3.313	Clear	No
	Col2α1 PP2	103.4	Yes	0.985	3.243	Clear	Yes

Table 3. Results after performing validation assay for primer pairs designed for reference genes, adipogenic genes, chondrogenic genes and osteogenic genes. Primer pairs that had an efficiency value superior to 110% were discard. Osteogenic gene primer pairs were not tested due to lack of suitable cDNA.

2.3.8 Gene Expression Analysis

Adipogenesis

In order to measure adipogenic gene expression of cell populations undergoing differentiation in AIM, we selected the specific markers Peroxisome Proliferator Activated Receptor Gamma (PPARG) and Lipoprotein Lipase (LPL), and used Glyceraldehyde 3-phosphate dehydrogenase (GADPH) and Eukaryotic translation initiation factor 1A (Eif1α) as housekeeping genes and did a qPCR analysis.

Results are shown in Figure 5 and Figure 6. The data for genetic expression has shown that cells of both *Acomys* and *Mus* when treated with AIM have upregulation of adipocyte specific genes. *Mus* displays an elevation in expression of PPARG and LPL at week 3, with these levels decreasing through weeks 4 to 5. The same behavior is seen in *Acomys*, with expression levels

increasing at week 3 followed by a subsequent decrease, but relatively to *Mus* the levels of these genes are lower in *Acomys*. These observations are in line with our histological stain results.

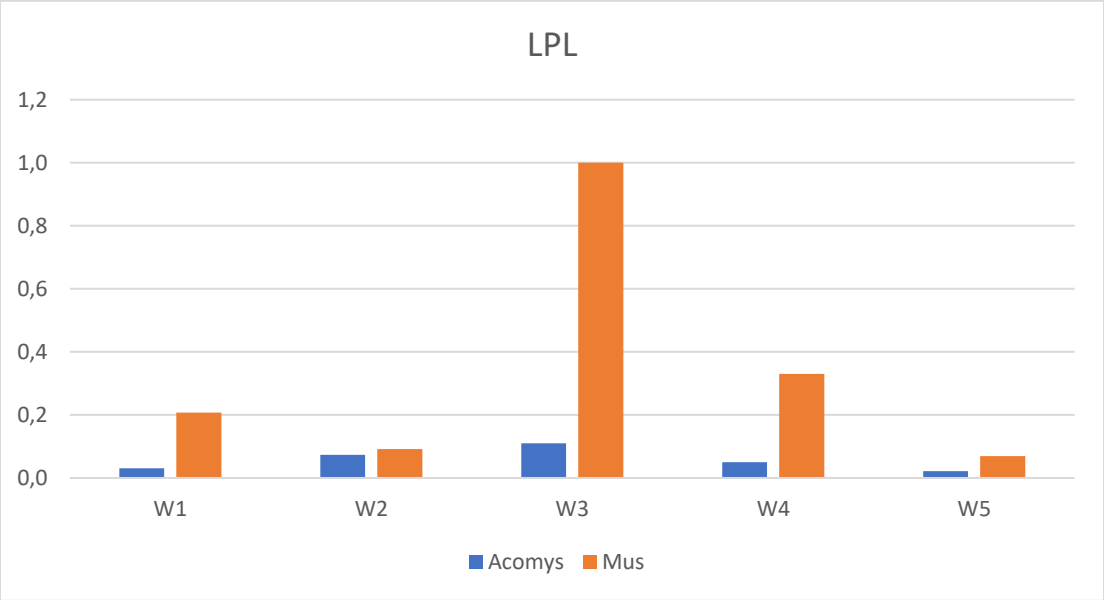

Figure 4. Relative Quantity (ΔCq) analysis for LPL in *Acomys* and *Mus* Adipogenic Cell Cultures (W1: 7 days; W2: 14 days; W3: 21 days; W4: 28 days; W5: 35 days)

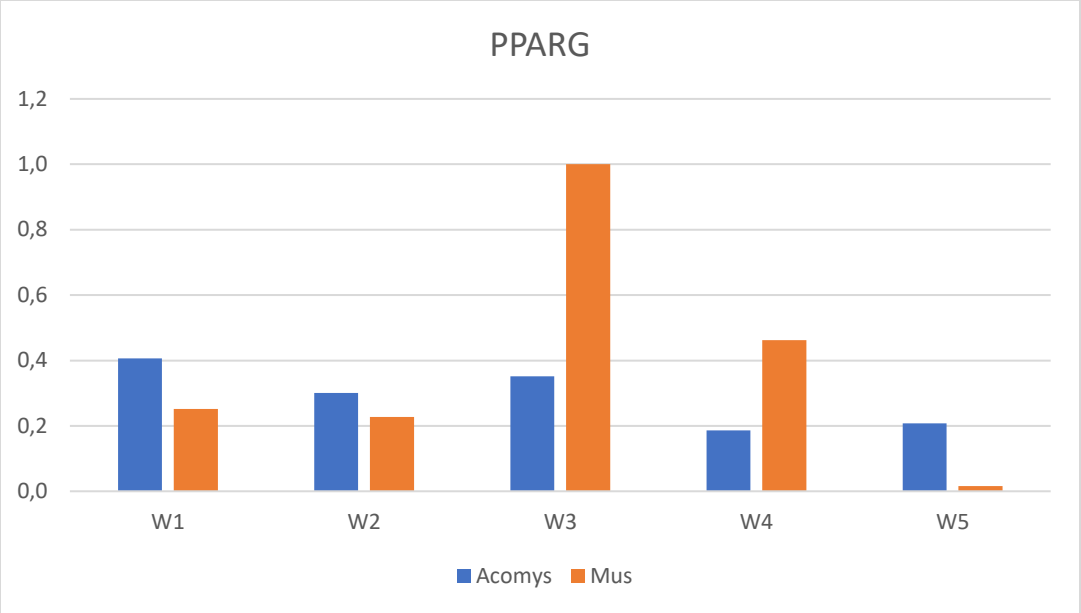

Figure 5. Relative Quantity (ΔCq) analysis for PPARG in *Acomys* and *Mus* Adipogenic Cell Cultures (W1: 7 days; W2: 14 days; W3: 21 days; W4: 28 days; W5: 35 days)

Chondrogenesis

Under the same parameters as the previous analysis, we constructed a genetic expression profile over time for the cells that underwent chondrogenesis, with the specific marker Collagen Type II alpha 1 chain (Col2α1), and used GADPH and Eif1a as housekeeping genes.

For the chondrogenic expression profile, seen in Figure 7, we observed that *Mus* does not display upregulation of Col2α1 throughout the 5 weeks, while *Acomys* shows a small increase in the target gene marker levels at week 3, followed massive upregulation of expression levels at week 5.

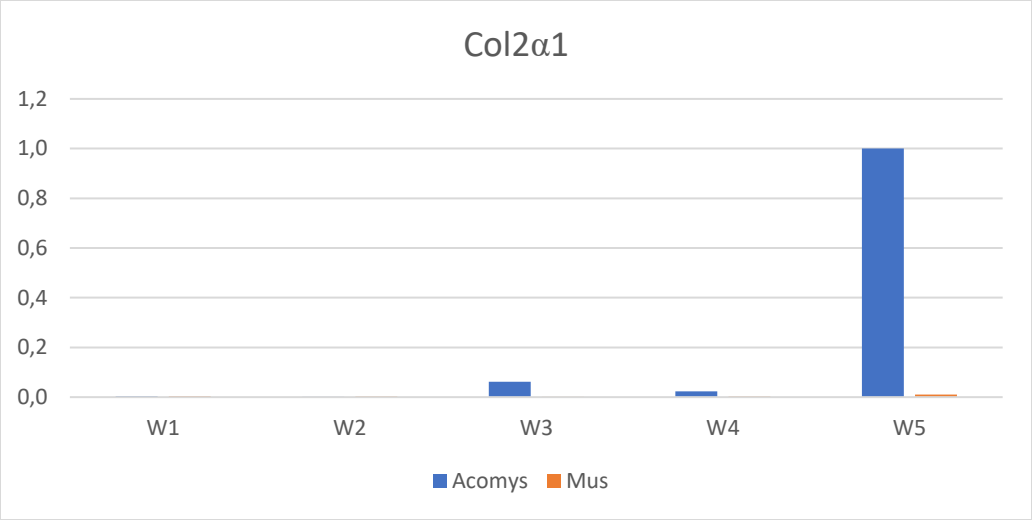

Figure 6. Relative Quantity (ΔCq) analysis for Col2α1 in *Acomys* and *Mus* Chondrogenic Cell Cultures (W1: 7 days; W2: 14 days; W3: 21 days; W4: 28 days; W5: 35 days)

2.4 Conclusions

We set out to identify whether MSC are present in the ears of *Mus* and *Acomys*, to characterize them, and to determine whether the behavior of these MSC compartments had any bearing on the different reaction to wounding in these 2 species: regeneration in *Acomys* vs. fibrotic scarring in *Mus*.

MSCs were originally isolated from bone marrow by selective plating on plastic substrates; in bone marrow, this method results in cultures highly enriched for MSC. Plating on plastic remains the standard for MSC isolation. When we applied this method to cells harvested from ears of *Mus* and *Acomys*, we were able to obtain proliferating populations of fibroblast like cells. *Acomys* cells proliferated faster that *Mus* cells, and the morphology of the cells differed somewhat between both species.

We sought to characterize the immunophenotype of the cell we had isolated. Using a commercial kit designed to detect the MSC in mice (CD29+, CD105+, Sca1+ and CD45-, we found that approximately 10% of the *Mus* cell population had a MSC immunophenotype. Therefore, by these criteria, *Mus* ear contains a subpopulation of MSCs. We assume the rest of the cells to be fibroblast like, with a relatively large population (approximately 40%) bearing Sca1+ and CD29+ markers.

The use of this commercial kit on *Acomys* cells had the uncertainty of the possibility that the antibodies raised against *Mus* markers would not react against the same markers in *Acomys*. Indeed, our FACS analysis labeled very few cells of *Acomys* with any combination of antibodies.

However, we did detect *Acomys* cells that were marked with either Sca1 or CD29, suggesting that these antibodies may be recognizing their intended epitopes in *Acomys*. However, very few cells (0.84%) had both markers. It therefore follows that there is no population bearing the MSC immunophenotype in *Acomys*. However, it is possible that the Sca1 and CD29 antibodies (raised against and validated for *Mus* epitopes) are cross-reacting with other, unknown epitopes in *Acomys*. In this case, our immunophenotyping results in *Acomys* would be inconclusive.

While there is a generally accepted immunophenotype for MSC, this population is operationally defined by their ability to differentiate into adipocytes, chondrocytes and osteocytes. Considering the possibility that *Mus* or *Acomys* ears could contain cells with multilineage differentiation potential regardless of whether their immunophenotype conforms to the accepted profile, we sought to test and compare the ability of *Mus* and Acomys ear cells to differentiate to these three cell fates.

Our *in vitro* differentiation experiments show that *Mus* and *Acomys* ear cell populations have different differentiation biases. *Mus* cells (but not *Acomys* cells) tend to differentiate to the adipocyte lineage when cultured in AIM, while *Acomys* cells (but not *Mus* cells) tend to differentiate to the chondrocyte lineage when cultured in CIM. These results were suggested first by analyzing the differentiated culture using commonly used histological stains (Oil Red and Alcian Blue). No staining for osteocytes (Alizarin Red) was detected for either species when cultured in OIM. The level of staining observed with Oil Red and Alcian Blue after 5 weeks of differentiation was relatively weak, suggesting that only a fraction of the cells in the starting culture were differentiating. It would be interesting to see the differentiation potential of a *Mus* populations sorted for the MSC immunophenotype in order to test and confirm whether this population has a strong MSC like differentiation behavior. In any case, our results were by expression analysis of adipocyte (LPL and PPARG) and chondrocyte (Col2α1) markers. Adipocyte markers were upregulated at later time points in *Mus* compared to *Acomys* when cultured in AIM. There was a slight discrepancy in our staining vs. expression analysis results in that maximum Oil Red staining was seen at 5 weeks, while maximum expression of adipocyte

markers was seen at week 3 and decreased thereafter. Similarly, the chondrocyte marker Col2α1was upregulated in week 3 of differentiation in *Acomys* cells, but not in *Mus* cells, when cells were cultured in CIM. In this case, maximum staining and maximum marker expression coincided at 5 weeks of culture in CIM.

Overall, we conclude that

1) a subpopulation of cells with the canonical MSC immunophenotype exists in *Mus* ears. However, we did not test whether this population is can indeed differentiate to the 3 fates (adipogenic, chondrogenic and osteogenic) required to confirm that they are indeed MSC.
2) We cannot confirm or rule out whether there is a population bearing the canonical MSC immunophenotype in Acomys ears.
3) Cultures obtained from *Mus* ears contain cells capable of differentiating into adipocytes.
4) Cultures obtained from Acomys ears contain cells capable of differentiating into chondrocytes. This observation is completely consistent with the confirmed ability of Acomys to regenerated cartilage in response to wounding.

2.5 Bibliographical References

Baghaban E. M., Bordbar S., "**Isolation and Characterization of the Progenitor Cells from the Blastema Tissue Formed at Experimentally-Created Rabbit Ear Hole**". *Iranian Journal of Basic Medical Sciences*, (2013) 16(2), pp. 109-115

Casanellas I., "The in vitro differentiation potential of *Mus musculus* vs. *Acomys cahirinus* ear cell populations" (Master Thesis, University of Algarve, 2015).

Dominici M., Le Blanc K., Mueller I., Slaper-Cortenbach I., Marini F. C., Krause D. S., Deans R. J., Keating A., Prockop D. J., Horwitz E. M., "**Minimal criteria for defining multipotent mesenchymal stromal cells**". *The International Society for Cellular Therapy position statement, Cytotherapy*, (2006), Vol. 8, No. 4, 315-317

Fiorina P., Jurewicz M., Augello A., Vergani A., Dada S., Selig M., Godwin J., Law K., Placidi R. N., Capella C., Rodig S., Adra C. N., Atkinson M., Sayegh M. H., Abdi R.,

"**Immunomodulatory function of bone marrow-derived mesenchymal stem cells in experimental autoimmune type 1 diabetes**", *Journal Immunology*, (2009), 183(2), pp. 993-1004

Herlofsen S. R., Kuchler A. M., Melvik J. E., Brinchmann J.E., "**Chondrogenic Differentiation of Human Bone Marrow-Derived Mesenchymal Stem Cells in Self-Gelling Alginate Discs Reveals Novel Chondrogenic Signature Gene Clusters**", *Tissue Engineering Part A*, 17(7-8), pp. 1003-1013

Keating A., "**Mesenchymal Stromal Cells: New Directions**", *Cell Stem Cell* (2012), 10, 709-716

Kolluri K. K., Laurent G. J., Janes S. M., "**Mesenchymal Stem Cells as Vectors for Lung Cancer Therapy**", *Respiration*, (2013), 85, pp. 443-451

Mundra V., Gerling C. I., Mahato R. I, "**Mesenchymal Stem Cell-Based Therapy**", *Mol. Pharm.*, (2013), 10(1), pp.77-89

Newman B., Gigout L. I., Sudre L., Grant M. E., Wallis G. A., "**Coordinated expression of matrix GLA protein is required during ossification for chondrocyte survival**". *The Journal of Cell Biology*, 153(3), pp. 659-666

Nombela-Arrieta C., Ritz J., Silberstein L. E., "**The elusive nature and function of mesenchymal stem cells**", *Nat Rev Mol Cell Biol.*, (2011), 12(2), pp.126-131

Rohban R., Pieber T. R., "**Mesenchymal Stem and Progenitor Cells in Regeneration: Tissue Specificity and Regenerative Potential**", *Stem Cells International*, (2017), pp. 1-16

Santos T. M., Percegona L. S., González P., Faucz F. R., Câmara N. O., Aita C. A., "**Expression of pancreatic endocrine markers by mesenchymal stem cells from umbilical cord vein**", *Transplant Proc*, (2010), 42(2), pp.563--5

Uccelli A., Moretta L., Pistoia V., "*Mesenchymal Stem Cells in Health and Disease*", *Nature Reviews Immunology* (2008), Vol. 8, 726-736

Vater C., Kasten P., Stiehler M., "**Culture Media for differentiation of mesenchymal stromal cells**", *Acta Biomaterialia*, (2011), 7, 463-477

Wang Y., Chen X., Cao W. Shi Y., "**Plasticity of mesenchymal stem cells in immunomodulation: pathological and therapeutic implications",** *Nature Immunology*, (2014), 15(11), pp. 1009-1016

Wei X., Yang X., Han Z., Qu F., Shao L., Shi Y., "**Mesenchymal stem cells: a new trend for cell therapy**", *Acta Pharmacologica Sinica*, (2013), 34, pp. 747-754

Chapter 3.

Is Telomerase involved in Ear Regeneration of *Acomys cahirinus*?

3.1 Introduction

In species with linear chromosomes, DNA ends are protected from genomic instability by telomeres. Telomeres are long complex ribonucleoprotein structures formed by extensive TACGGG hexameric repeats. In order to divide, a cell *Mus*t first replicate its entire genome. Organisms with linear chromosomes face the problem of how to replicate chromosome ends. During replication, DNA polymerase catalyzes the addition of a nucleotide to the 3'OH of the preceding nucleotide in a 5' to 3' direction using the complementary DNA strand as a template. Because DNA replication of the lagging strand uses Okazaki fragments to provide 3'OH termini, the replication machinery cannot replicate the 3' end of the chromosome, leaving a 3' single strand overhang at the end of the chromosome that is degraded. As a result, the chromosome is shortened by an average of 50 kb per cycle. This is known as the end-replication problem. The observation that normal, differentiated cells in culture enter replicative senescence after a characteristic number of cell divisions (Hayflick limit) (Calado et. al. 2013, Shay et. al. 2000), a phenomenon that is explained by telomeres shortening to the point that chromosome stability can no longer be sustained. Telomere attrition can result in chromosomal instability and aneuploidy, which can contribute to the development of cancer if tumor suppressor alleles are lost and/or generation of fusion genes with altered functions (Li et. al. 2009).

In most adult somatic cells undergoing continuous replication, telomere shortening is unavoidable. However, in certain cell types, such as stem/progenitor cells and some cancer cells, telomere length is maintained due to upregulation of expression of the enzyme telomerase. Telomerase is a holoenzyme formed by two main components, the telomerase reverse transcriptase (TERT, encoded by the gene *Tert* (Blasco et al 2005), and an RNA component (TERC).

Telomerase catalyzes telomere extension; TERC provides a template for hexameric repeats. Telomerase recognizes the 3-OH group of the G-band overhang as a binding region, and it is from there that it initiates de novo addition of TCAGGG repeats, thus elongating chromosome ends (Blasco et al 2005). Telomeres also prevent the double strand break repair machinery from

recognizing DNA chromosome ends as breaks (Li et al 2009, Flores et al 2006). The telomere maintenance system, or more accurately telomerase, have been proposed to play a major role in organism ageing, cancer development and, of more relevance for our line of work, in regeneration events (REF).

Tert gene up-regulation is essential in proliferating cell populations, and it has been observed that in species with strong regenerative capability, such as in the zebrafish (*Danio rerio),* there is a constitutively abundant telomerase activity in somatic tissues from embryos to aged adults. In many invertebrate and vertebrate aquatic species that show increased regenerative capacity, such as the Japanese medaka fish (*Oryzias latipes),* a well characterized model for studies of the telomere maintenance system there is an upregulation of TERT during regeneration events (Anchelin et al 2010, Elmore et al 2008).

Zebrafish regenerates many of its tissues and structures after physical injury, and the process results in a functional structure without evidence of fibrotic scar. This regenerative event proceeds through a transient blastema stage, a hallmark of epimorphic regeneration. It has been show in Zebrafish (*danio rerio*) that TERT is upregulated during tissue regeneration events (Anchelin et al 2010, Elmore et al 2008).

The importance of telomerase for regeneration is not limited to skin tissue, but other vital organs, such as heart, where reports indicate that after heart injury, absence of telomerase activity drastically impairs proliferation, there is a lack of apoptosis protection and cells display a senescent phenotype (Flores et al 2015). Another study in mice heart regeneration determined that telomere shortening negatively impacts cardiomyocyte cell-cycle arrest, and results in impaired repair of heart lesions (Aix et al 2016). In this study, it was seen that telomere shortening results in up-regulation of cell-cycle inhibitor p21, and inhibition of cardiomyocyte proliferation. In contrast, mice with a knockout for p21 ($p21^{-/-}$) displayed robust proliferation of cardiomyocytes, whilst mice with the RNA template knockout ($Terc^{-/-}$) showed severe telomere shortening, shorter lifespans, upregulation of p21 and significantly lower proliferation of cardiomyocytes when compared to wild-type mice. These findings highlight an important role of the telomere maintenance system in injury response events in mammalian heart (Aix et al 2016).

We set out to answer a simple question: is TERT upregulated during regeneration of full thickness ear pina wounds in *Acomys cahirinus*?

3.2 Materials and Methods

3.2.1 Ear Wound Regeneration Assay

In order to obtain tissue samples representative of key points in the regenerative process, animals we anesthetized with isofluorane, and 4 mm full thickness circular ear wounds were made bilaterally to *Acomys* or *Mus* individuals using a Biopsy Punch (Miltex 33-34). The resulting ear pinna tissue disc was flash frozen and stored at -80C, or, alternatively, processed immediately. This sample provided TERT expression levels in uninjured tissue.

Animals were kept in isolated clean boxes and allowed to regenerate (*Acomys*) or heal (*Mus*) their wounds. After 30 days, *Acomys* wounds had formed a clearly visible blastema, while *Mus* wounds had healed the borders of their wounds with fibrotic scarring.

A group of animals for each species were chosen randomly, anesthetized and their ears harvested. These samples were further microdisected into 2 compartments called ‘ring’ and ‘rest’. A 1 mm thick circular ring of tissue encompassing the blastema (in *Acomys*) or the fibrotic scar (in *Mus*) was harvested by microdissection, flash frozen and stored at -80C (‘ring’), or, alternatively, processed immediately. These samples provided a measure of TERT levels in the blastema of during *Acomys* regeneration and in the corresponding region in *Mus* ears (which presented scarred tissue) at the 30 day after injury time-point. The remaining ear tissue (after the ‘ring’ tissue was microdissected was also harvested (‘rest) and were used to measure TERT levels in tissue neighboring the wound but not itself undergoing regeneration or scarring.

A second group of animals were allowed to continue regenerating (*Acomys*) until the wound was completely closed (approximately 60 days after injury). At this time, ears were harvested and further microdisected into 2 compartments called ‘regenerated disc’ and ‘rest’. The regenerated disc consisted in the 4-mm diameter circle of regenerated tissue corresponding to the original disc cut to create the initial wound. The remaining ear was called ‘rest’. Both samples were flash frozen and stored at -80C.

We did not collect a 60 day time point equivalent for *Mus*, as, due to the fact that *Mus* does not regenerate and healing is complete at 30 days post-injury, the resulting compartment would be similar to those already obtained at 30 days post-injury.

3.2.2 Tissue Harvest and RNA Extraction

Final optimized protocol is extensively described in the **Results and Discussion** section, under "Optimization of a Total RNA Extraction protocol from tissues of *Acomys cahirinus*"

3.2.3 RT-qPCR

Total RNA (500 µg) was reverse transcribed (resulting in a RT+ cDNA fraction) using an iScript cDNA Synthesis Kit (Bio-Rad, 170-8891), following the manufacturer's instructions. A control reaction was set up without reverse transcriptase (RT- cDNA fraction). Reactions were conducted in a C1000 Touch Thermal Cycler (Bio-Rad). Quantitative PCR was performed using SSoFast EvaGreen Supermix (Bio-Rad, 172-5201) in a 96 well plate format on a CFX96 Real-Time PCR System (Bio-Rad).

3.3 Results and Discussion

3.3.1 Optimization of a Total RNA Extraction from Ear Tissue

In an initial attempt at total RNA extraction from *Acomys* tissue, two commercial column kits were used: NZYTech (NZY Total RNA Isolation kit, MB13402) and Qiagen (RNeasy Mini Kit, Cat. No. 74104).

Prior to initiating the column kit extraction protocol, fresh tissue or frozen tissue was placed in a petri dish, on ice, and cut into a 'pulp' using sterile scalpel blades. The tissue was transferred into a DEPC-treated Eppendorf and the lysis buffer from the column kit was added, with volume varying depending on protocol and volume of tissue and manufacturers instruction were followed exactly. An aliquot of 2 µl was taken to analyze RNA quality and quantity, and the remainder of the RNA extract was stored at -80ºC. These procedures resulted in

An average RNA concentration of 300 ng/µl and an acceptable absorbance ratio A260/A280 (1.9 - 2.2), measured by NanoDrop (Thermo Scientific 2000c), subsequent analysis by Experion (Bio-Rad, #700-7000) showed that the samples were very degraded, with RQI varying between 4.0 and 5.0.

Given that the acceptable RQI value for genetic expression analysis by RT-qPCR is of 7.0 or above, we set out to optimize a protocol for the total extraction of RNA from *Acomys* tissue. We therefore varied a number of parameters of the extraction protocol.

Initially we reasoned that because ear tissue is highly fibrous, incomplete disruption of the tissue prior to addition of the extraction buffer might be resulting in incomplete neutralization of endogenous RNAses and therefore, RNA degradation.

Several procedures were devised and tested:

Procedure 1: Mechanical maceration of the tissue with scalpels followed by proteinase K digestion during 30 minutes.

Procedure 2: Freezing of tissue with liquid nitrogen, mechanical maceration with mortar and pestle, followed by proteinase K digestion for 30 minutes.

Procedure 3: Mechanical maceration of the tissue with scalpels, followed by further maceration using a Mini Potter Tissue Grinder 0,1 mL (GPE Scientific 20404F), while tissue is submerged in the column kit's lysis buffer.

Procedure 4: Mechanical maceration of the tissue with scalpel blades followed by NZYol (nzytech, Cat No. MB18501) RNA extraction (a phenol based extraction followed by precipitation with isopropanol).

Procedures 1, 2 and 3 resulted in complete digestion of the tissue but high levels of RNA degradation. We concluded that prolonged incubation in proteinase K, or use of a Mini Potter Tissue Grinder 0,1 mL (GPE Scientific 20404F), while efficiently digesting the tissue, allowed an ample window for RNAses to act.

Procedure 4, a phenol based RNA extraction method, was the only method that resulted in a larger yield of RNA with better quality. However, Experion analysis indicated that RIN values (5 to 6.5), while improved, were still relatively low. Furthermore, initial RT-qPCR assays using

these samples indicated gDNA contamination. Procedure 4 was therefore modified into Procedure 5.

Procedure 5: Mechanical maceration of the tissue using scalpel blades, followed by phenol extraction (NZYol). However, the aqueous phase was not precipitated with isopropanol as in Procedure 4, but loaded onto a RNA affinity binding column (Quick-RNA MiniPrep, Cat. No. R1054). DNAse I solution was added to the column, after which the column was washed and RNA eluted.

Procedure 5 resolved our issues with gDNA contamination, and provided RQI levels > 6 in Experion analysis, which was closer (although did not meet) the level of RQI = 7 recommended by MIQUE.

Procedure 6: We therefore developed a final procedure based on a newly acquired equipment called a Bullet Blender. This procedure involves putting the sample in a tube with a phenol based extraction buffer and a small number of solid beads that are machine vibrates at high speed, resulting in quick and thorough homogenization of the samples and reducing time of extraction. Both metallic and ceramic beads were tested. Ceramic beads proved preferable to metallic beads in several ways: a) they disrupted the tissue more efficiently; b) leftover sample 'sticked' less to ceramic beads than metallic beads and c) the aqueous phase was translucent (as opposed to yellowish when metallic beads were used). The aqueous phase was subject to isopropanol precipitation and the RNA resuspended in DEPc treated water. Finally, DNAse I was added to the preparation, incubated at 37C for 10 minutes and inactivated by adding 0.1 mM EDTA and incubating at 75C FOR 15 minutes. This procedure consistently gave good yields and RIN values between 6.6 and 8.7.

3.3.2 Validation of Primer Pairs

Four primer pairs designed to detect TERT expression in both *Mus* and Acomys were designed using the same criteria as in Chapter 2 (see Table 4).

Target Gene	Sequences
TERT PP1	FP: GTCTCTGGGGTACCAGGCA RP: GATCCTCTCCCTCAGACGGT
TERT PP2	FP: GTAAGAGTGTGTGGAGCAAGC RP: GCAGATGGGCATGGCTGG
TERT PP3	FP: GGGCCTATGATGCCATCCC RP: ATGGCTGGAGGTCAGAGAGG
TERT PP4	FP: CCACCCTCTCTGACCTCCAG RP: GCAGGAAGAAGTCAAACAGGC
TERT PP5	FP: CCTGTTTGACTTCTTCCTGCAC RP: GGAAGTCATCAACAAAACGTAAAAG

Table 4. Primer pairs for RT-qPCR (FP: forward primer; RP: reverse primer)

Primer pairs were validated following the methodology described in Chapter 2 using total RNA samples extracted from mouse ES cells, known to express relatively high levels of TERT. Results are shown on in Figure 8 and Table 5.

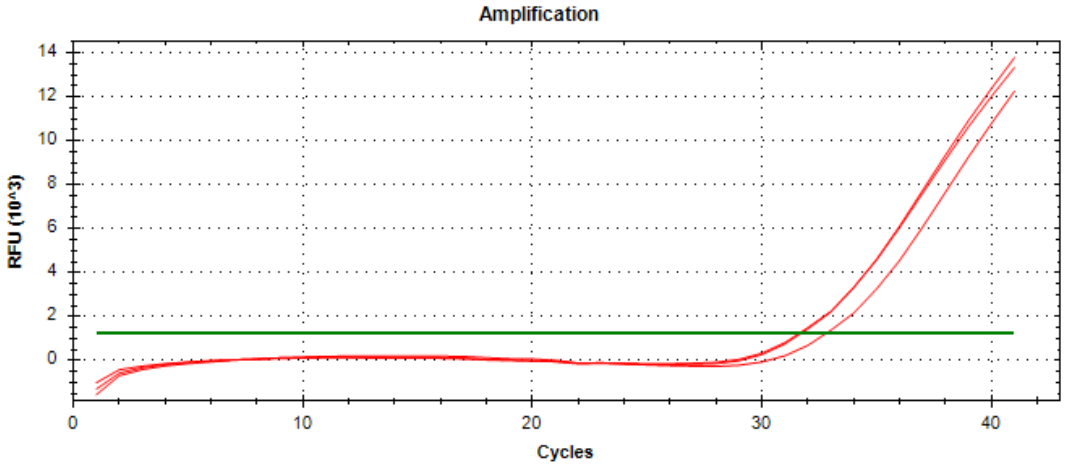

Figure 7. Red lines represent amplification signal for TERT on mESC RNA.

Target Gene	Efficiency (%)	Specific?	R^2	Slope (Cq/Log(SQ))	NRT/RT- and NTC	Usable?
TERT-PP1	101.5	Yes	0.993		Clean	Yes
TERT-PP2	Discarded: unacceptable level of amplification of NRT					No
TERT-PP3	179.7	Yes	0.990		Clean	No
TERT-PP4	97.3	Yes	0.980		Clean	Yes
TERT-PP5	Not Tested					

Table 5. Results of the validation of primer pairs for TERT on *Mus* mESC RNA. (NRT/RT-: No Reverse Transcription; NTC: No template Control)

3.3.3 Gene Expression Analysis

We set out to perform RT-qPCR to characterize TERT expression in response to wounding in *Acomys* versus *Mus*. We used GADPH and Eif1α as our reference genes, and mESC RNA as a TERT expression positive control.

Using RNA obtained with Procedure 6, we were unable to see any amplification signal for our target gene (TERT). Notably, we did get signal for mouse embryonic stem cell (mESC) cDNA

included in the plate as a positive control, showing that the lack of signal in our samples was not due to a faulty qPCR technique (Figure 9). Unexpectedly, however, we did not amplify any signal from or our reference genes (GADPH and Eif1a) on any of the samples from either species.

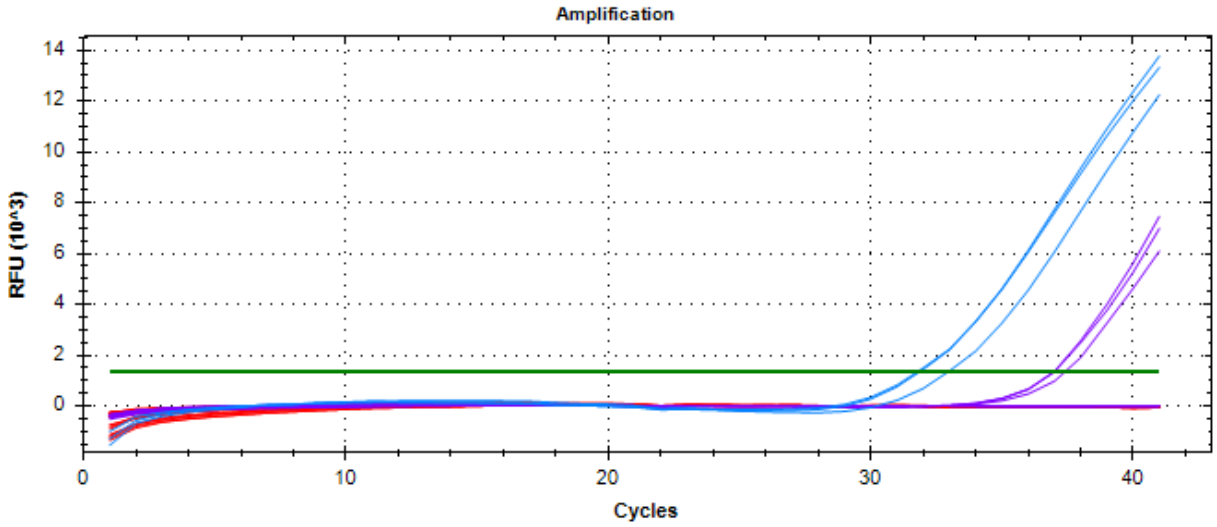

Figure 8. RT-qPCR results for TERT amplification signal on *Acomys* compartment samples and mESc control sample. Blue line is relative to GADPH amplification signal for mESC. Purple amplification line is GADPH signal in our sample. Red line is the amplification signal for TERT.

We hypothesized that there could be some unidentified inhibitor agent present in our samples. In order to test this, we set up an experiment in which we used two different samples (a and b). Sample a) was our hypothetic, inhibitor containing RNA sample from which we could not amplify signal with our reference genes. Sample b) was a previously generated 'positive control' RNA sample from which we had successfully amplified signal in the past for our reference genes (in particular, RNA obtained from cell line ATDC5, which amplified both GADPH and Eif1a efficiently).

We set up an qPCR experiment for GADPH for three samples: 1) our 'inhibited' RNA, 2) the 'positive control' RNA and 3) a 1:1 mixture of both samples. We reasoned that if an inhibitor

was present in sample 1, the result obtained in sample 3 would be informative. Amplification of signal in sample 3 would suggest that no inhibitor was present. On the contrary, lack of amplification in sample 3 would indeed suggest the presence of an inhibitor in sample 1.

Results are shown in Figure 9. GADPH was clearly amplified in sample 3), albeit with a slightly higher Cq, reflecting the 1:1 dilution of sample 1 to sample 3. Therefore, we conclude that our samples do not contain a PCR inhibitor.

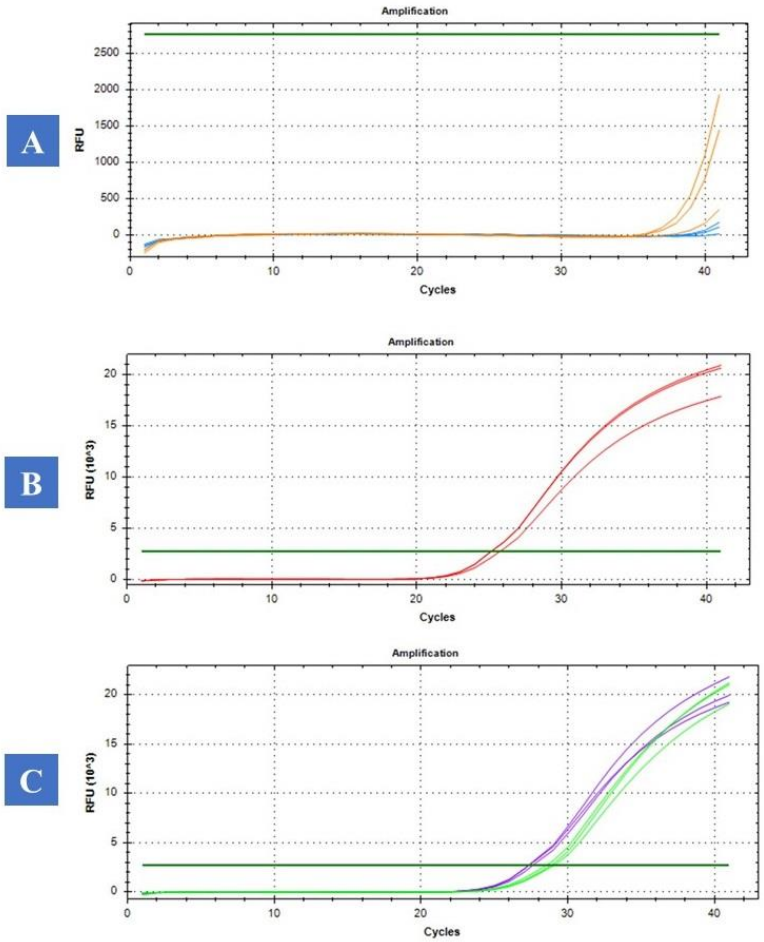

Figure 9. A) Amplification levels of GADPH for sample 1), orange curves are relative to sample extracted ceramic beads, while blue are for RNA extracted with steel beads; B) Amplification signal for GADPH on mESC; C) Purple curves represent GADH amplification level for a 1:1 mixture of RNA from mESC and RNA obtained with the ceramic bead maceration. Green curves represent amplification of TERT in a 1:1 mixture of RNA from mESC and RNA obtained with steel bead maceration.

These results led us to discard the presence of inhibiting agents in our RNA extracts since signal was observed for both mixtures of working cDNA with RNA from the metallic bead extract and the mixture of working cDNA and ceramic bead RNA extract.

3.4 Conclusions

Despite intense effort and repeated attempts, we were unable to measure expression of TERT by RT-qPCR in ear tissues of *Mus* and *Acomys* subject to wounds and allowed to heal for 30 days (*Mus*) or regenerate for 60 days (*Acomys*). Ultimately, we do not have a satisfactory explanation for this, but a number of points are worth highlighting.

First, we cannot interpret our lack of signal to be due to the fact that TERT is not expressed at all in uninjured, regenerating, healed or regenerated tissue due to the fact that signal was not obtained either when using primers against housekeeping genes such as GADPH, ACTB and EIF1a, which can be reasonably be expected to be expressed at high levels in ear tissue. Therefore, the question of whether TERT is (or not) expressed in ear tissue remains unanswered.

Second, the lack of qPCR signal is not due to faulty technical execution of the qPCR procedure, as all primer validation experiments and all measurements carried out in Chapter 2 were successful.

Third, failure to detect TERT in ear tissue was not due to an unexpected problem in a particular experiment. The measurement was attempted multiple times with several RNA preparations performed independently. In particular, in our attempt to detect TERT in ear tissue, we added cDNA obtained from mouse ES cells to our qPCR plates as a positive control and obtained good amplification.

Third, the results are not due to poorly designed TERT primers, as these primers were successfully used to detect TERT expression and validated in mouse ES cells. The same can be said of the primers used to detect expression of housekeeping genes, which were the same used successfully in Chapter 2.

We suspect that the problem lies in the quality of the RNA extract obtained from ear tissue. As described above, we invested significant time and effort in fine-tunning a RNA extraction

procedure. Obtaining good quality RNA proved unexpectedly difficult. Procedures that work in many tissues, namely mechanical dissagregation followed by phenol based extraction or commercial column based kits resulted in low yields, poor integrity and variable reproducibility. Introduction of a bead basher based technique improved matters in terms of yield and integrity, but RIN values remained over 6 but under 7. Attempts to determine if the problem was due to an unidentified PCR inhibitor present in the RNA extract were equally inconclusive. Consultation with a collaborating lab (Dr. A. Seifert, University of Kentucky, USA) who has successfully done qPCR on ear tissue did not reveal what could be the problem. Seifert's group utilizes a bead bashing protocol very similar to the one we developed. This technical problem remains unsolved.

Interestingly, while this work was being executed, Dr. Seifert's group completed an RNAseq transcriptional profile of regenerating ear of *Acomys* with healing ear of *Mus* at 5 day intervals up to 20 days post-injury. In their data set, TERT expression (see Figure 11) was found at low levels in uninjured tissue and moderately upregulated in both species after wounding.

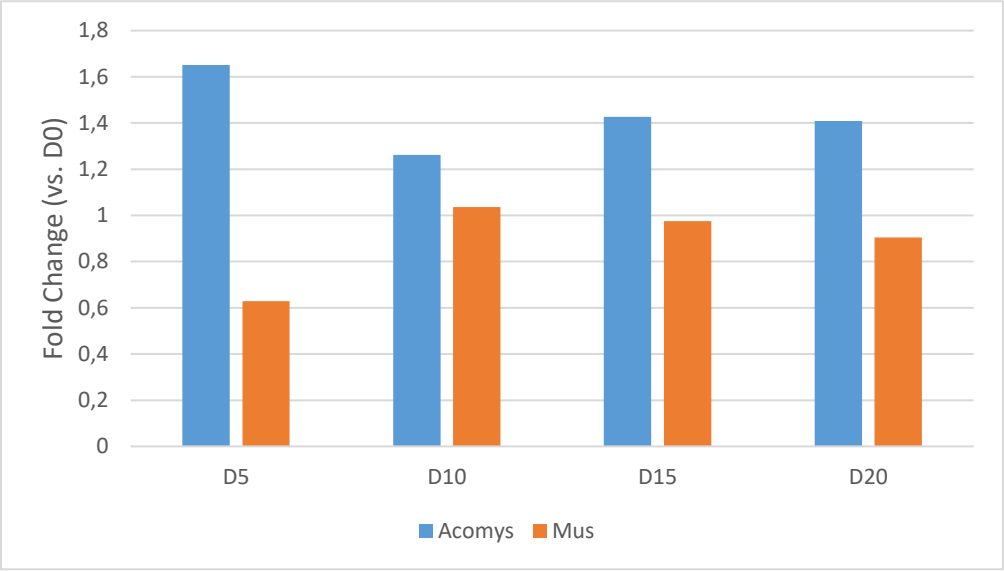

Figure 10. Preliminary data relative to TERT Expression on *Acomys* ear tissue post-injury. Data provided to us by Ashley Seifert, University of Kentucky, USA (D5: day 5; D10: day 10; D15: day 15; D20: day 20).

Levels were slightly higher in *Acomys* than *Mus* for all time points, particularly at day 5 post-injury, where TERT in *Acomys* was increased 1.6x compared to day 0, while *Mus* was upregulated 1.03x. The low levels of expression did not allow for statistical analysis of the differences. This result suggests several things:

1) TERT expression is low in uninjured tissue. This level of expression might be general transcriptional noise throughout the entire tissue, or, alternatively, suggest that there is high level of expression in a small number of cells. Given that TERT expression is a hallmark of high potency stem cells, this is consistent with the idea of a small population of stem cells residing in uninjured tissue.
2) Compared with expression levels at day 0, TERT expression seems to be upregulated upon wounding in both species. At day 5, TERT levels seem to be higher in *Acomys* than *Mus*. The fold increase (1.6x in *Acomys* and 1.03x in *Mus* is robust enough to believe that the increase is significant. It is not clear that the levels are statistically different between

Mus and *Acomys*. If indeed the observed upregulation reflects a mobilization of a small stem cell compartment, said mobilization occurs in both species.

3) Levels of TERT continue upregulated throughout days 10, 15 and 20. Levels between *Mus* and *Acomys* seem similar. Therefore, there is no correlation of the behavior of TERT expression with regeneration in *Acomys* vs fibrotic scarring in *Mus*.

Overall, the transcriptomic profiling results obtained by Seifert's group seem to suggest that the proliferation required to regenerate missing tissue in *Acomys* is not dependent on a massive upregulation of TERT, as observed in the zebrafish system. TERT expression is high in ES cells, induced pluripotent stem cells, spermatogonial stem cells (or somatic stem cells in general). If it is accepted that TERT is a marker of highly potent cells, then we would conclude that regeneration in *Acomys* is not based on the mobilization of an endogenous compartment of quiescent stem cells of high potency. If one hypothesizes that *Acomys* regeneration involves de-differentiation, said de-differentiation does not result in the creation of a cell compartment with high potency. It would be interesting to solve our qPCR technical problems to complete our measurement and compare our results with Seifert's transcriptional profile for TERT. Another interesting avenue would be to detect TERT by immunohistochemistry to determine the existence of possible 'clusters' of TERT positive cells in particular regions or niches of the tissue, and analyze their behavior in response to wounding.

3.5 Bibliographical References

Aix E., Gutiérrez- Gutiérrez Ó., Sánchez-Ferrer C., Aguado T., Flores I., "**Postnatal telomere dysfunction induces cardiomyocyte cell-cycle arrest through p21 activation**", *The Journal of Cell Biology* (2016), Vol. 213 (5), pp. 571-583

Anchelin, M., Murcia, L., Alcaraz-Pérez, F. A., García-Navarro, E. M., Cayuela, M. L., (2010) "**Behaviour of Telomere and Telomerase during Aging and Regeneration in Zebrafish**" *PLoS ONE* 6(2): e16966. Doi:10.1371/journal.pone.0016955

Armstrong, L., Lako, M., Lincoln, J., Cairns, P. M., Hole, N. "**mTert expression correlates with telomerase activity during the differentiation of murine embryonic stem cells**" *Mechanisms of Development*, (200) 97, pp. 109-116

Blackburn, E. H. and Gall J. G.,"**A Tandemly Repeated Sequence at the Termini of the Extrachromosomal Ribosomal RNA Genes in Tetrahymena**". *Journal of Molecular Biology* (1978) 120, pp. 33-53

Blasco, M. A. "**Telomeres and Human Disease: Ageing, Cancer and Beyond**". *Nature Reviews Genetics* (2005) Vol. 6, pp 611-620

Bustin S. A., Benes V., Garson J. A., Hellemans J., Huggett J., Kubista M., Mueller R., Nolan T., Pfaffl m. W., Shipley G. L., Vandesompele J., Wittwer C. T., "**The MIQE Guidelines: Minimun Information for Publication of Quantitative Real-Time PCR Experiments**", *Clinical Chemistry* (2009), 55:4, 611-622

Calado T.R., Dumitriu B. "**Telomere Dynamics in Mice and Humans"**, *Seminars in Hematology* (2013) Vol 50 (2), pp 165-174

Elmore L. W., Norris M. W., Sircar S., Bright A. T., McChesney P. A., Winn R. N., Holt S. E., (2008) "**Upregulation of Telomerase Function During Tissue Regeneration**". *Society for Experimental Biology and Medicine*, pp 958-967, doi:10.3181/0712-RM-345

Flores I., "**Telomerase is Essential for Zebrafish Heart Regeneration**". *Cell Reports* (12) (2015), pp. 1691-1703

Flores I., Benetti R., Blasco M. A., "**Telomerase regulation and stem cell behavior**". *Current Opinion in Cell Biology* (2006), 18, pp. 254-460

Greider, C. W. and Blackburn E. H. "**Identification of a Specific Telomere Terminal Transferase Activity in Tetrahymena Extracts**". *Cell* (1985) 43, pp. 403-413

Haubner B. J., "**Functional Recovery of a Human Neonatal Heart After Severe Myocardial Infarction**" *Circ. Res.* (2016) (!!!)

Kumar M., Lechel A., Gunes Ç., "**Telomerase: The Devil Inside**". *Genes* (2016), 7, 43, doi:10.3390/genes/7080043

Lange T., "**Shelterin: the protein complex that shapes and safeguards human telomeres**" *Genes & Development* (2005), 19, pp. 2100-2110

Li P. L. and Norbury C. J. "**Telomere Maintenance: all's well that ends well**". *Arch Toxicol* (2009) 83, pp. 407-416

Marión R. M., Blasco M. A., "**Telomeres and Telomerase in Adult Stem Cells and Pluripotent Embryonic Stem Cells**" *The Cell Biology of Stem Cells* (9), (2010), pp. 118-131

Martínez, P., Blasco, M. A. "**Replicating through telomeres: a means to an end**". *Trends in Biochemical Sciences* (2015) Vol. 40(9), pp 504-515

Poss, K. D. "**Advances in understanding tissue regenerative capacity and mechanisms in animals**". *Nature Reviews*, (2010), Vol 11, pp 710-722

Rodríguez A., Rodríguez M., Córdoba J. J., Andrade M. J., "**PCR Primer Design**", *Methods in Molecular Biology*, Vol. 1275 (Chp. 3), 31-56

Shay J. W., Wright W. E., "**Hayflick, his limit, and cellular ageing**" *Nature Reviews Molecular Cell Biology* (2000), pp. 72-76

Trivanovic D., Krstic J., Jaukovic A., Popovic B., Djordjevic I., O., Kukojl T., Obradovic H., Mojsilovic S., Santibanez J. F., Bugarski D., "**Correlation between telomere maintenance and stemness of mesenchymal stem/stromal cells**" *Telomere and Telomerase* (2016) (3) e1184. Doi:10.14800//tt.1184

Annexes

Supplementary Figures

Supplementary Figure 1. Postnatal development of *Acomys cahirinus*. a) Two day old pup; b) 1 week old pup; c) 4 week old juvenile; d) 3 month old adult

Validation of Primer Pairs

In order to guarantee that data relative to genetic expression is significant, that is not influenced by background, and specific to the genes targeted by primers, the primers were assayed in order to determine their efficiency and specificity. This was done by testing primers pairs on cDNA produced by reverse transcription of RNA extracted from tissues that are known to express the genes targeted. RNA extraction was meticulously done in order to obtain pure Total RNA, and subsequently was treated with an in-solution DNase I digestion step (Materials and Methods) in order to guarantee no genomic contamination.

Primer pair validation takes into account two main parameters, primer pair efficiency and specificity. The efficiency parameter relates to the PCR reaction in itself. Theoretically, a PCR reaction would have an efficiency of 100%, with DNA template being exactly duplicated in each

cycle of the reaction. However, in practice, this may not be the case, and efficiency *Mus*t be assayed. Specificity of primer pairs is determined true melting curve (automatically given by CFX-96 software), the curve is a result of fluorescence readings for given points, in gradually higher temperature cycles.

Primer pairs that have an efficiency within the 90-110% interval and display only one peak in melt curve analysis are regarded as validated and can be used for RT-qPCR assays.

In order to analyze these parameters for a given primer pair, an RT-qPCR is done. For that, the cDNA resultant of reverse transcription is serially diluted by a 10-fold factor so that a plot may be drawn and efficiency calculated. The inputs, in 8 µl, were as follows:

Diltutions	1º	2º	3º	4º
cDNA input concentration (ng/µl)	1,25	0,125	0,0125	0,00125
Total cDNA per well (ng)	10	1	0,1	0,001

The RNA used for cDNA synthesis for the validation of primer pairs had an RQI value of 7 or more for all instances.